

Using an integrative taxonomic approach to delimit a sibling species, *Mycetomoellerius mikromelanos* sp. nov. (Formicidae: Attini: Attina)

Cody Raul Cardenas¹, Amy Rongyan Luo², Tappey H. Jones³, Ted R. Schultz⁴ and Rachelle M.M. Adams^{1,4}

¹ Department of Evolution, Ecology and Organismal Biology, The Ohio State University, Columbus, OH, United States of America

² Department of Ecology & Evolutionary Biology, University of Tennessee Knoxville, Knoxville, TN, United States of America

³ Department of Chemistry, Virginia Military Institute, Lexington, VA, United States of America

⁴ Department of Entomology, National Museum of Natural History, Smithsonian Institution, Washington, District of Columbia, United States of America

ABSTRACT

The fungus-growing ant *Mycetomoellerius* (previously *Trachymyrmex*) *zeteki* (Weber 1940) has been the focus of a wide range of studies examining symbiotic partners, garden pathogens, mating frequencies, and genomics. This is in part due to the ease of collecting colonies from creek embankments and its high abundance in the Panama Canal region. The original description was based on samples collected on Barro Colorado Island (BCI), Panama. However, most subsequent studies have sampled populations on the mainland 15 km southeast of BCI. Herein we show that two sibling ant species live in sympatry on the mainland: *Mycetomoellerius mikromelanos* Cardenas, Schultz, & Adams and *M. zeteki*. This distinction was originally based on behavioral differences of workers in the field and on queen morphology (*M. mikromelanos* workers and queens are smaller and black while those of *M. zeteki* are larger and red). Authors frequently refer to either species as “*M. cf. zeteki*,” indicating uncertainty about identity. We used an integrative taxonomic approach to resolve this, examining worker behavior, chemical profiles of worker volatiles, molecular markers, and morphology of all castes. For the latter, we used conventional taxonomic indicators from nine measurements, six extrapolated indices, and morphological characters. We document a new observation of a Diapriinae (Hymenoptera: Diapriidae) parasitoid wasp parasitizing *M. zeteki*. Finally, we discuss the importance of vouchering in dependable, accessible museum collections and provide a table of previously published papers to clarify the usage of the name *T. zeteki*. We found that most reports of *M. zeteki* or *M. cf. zeteki*—including a genome—actually refer to the new species *M. mikromelanos*.

Submitted 16 December 2020

Accepted 26 May 2021

Published 24 June 2021

Corresponding authors

Cody Raul Cardenas,
cardenas.61@buckeyemail.osu.edu
Rachelle M.M. Adams,
adams.1970@osu.edu

Academic editor
Joseph Gillespie

Additional Information and
Declarations can be found on
page 30

DOI 10.7717/peerj.11622

© Copyright
2021 Cardenas et al.

Distributed under
Creative Commons CC-BY 4.0

OPEN ACCESS

Subjects Biodiversity, Entomology, Taxonomy, Zoology

Keywords Integrative taxonomy, Cryptic species, Formicidae, Myrmicinae, Attine, Attina, Fungus-growing ants

INTRODUCTION

Fungus-growing ants (Hymenoptera: Formicidae: Attini: Attina; [Ward et al., 2015](#)), referred to as “attine” ants, cultivate mutualistic fungus gardens using sophisticated agricultural practices ([Weber, 1958a](#)). This clade of 240 extant described species has been tending and feeding cultivated fungi for ca. 60 million years ([Branstetter et al., 2017](#)). Because fungus-growing ants have been focal taxa of studies in evolutionary biology, including mating systems ([Baer & Boomsma, 2004](#); [Boomsma, 2007](#)), symbiotic networks ([Mueller, Rehner & Schultz, 1998](#); [Currie, Mueller & Malloch, 1999](#)), social parasitism ([Adams et al., 2013](#)), host fidelity ([Mehdiabadi et al., 2012](#)), and genome evolution ([Nygaard et al., 2016](#)), it is imperative that the taxonomy of attine ants accurately reflects their evolutionary history. Diverse studies indicate the existence of many undescribed species ([Schultz & Meier, 1995](#); [Schultz, Bekkevold & Boomsma, 1998](#); [Rabeling et al., 2007](#); [Schultz & Brady, 2008](#); [Mehdiabadi et al., 2012](#); [Ješovník et al., 2013](#); [Sosa-Calvo et al., 2018](#); [Solomon et al., 2019](#)) and alpha-taxonomic work has been steadily carried out by many taxonomists ([Mayhé-Nunes & Brandão, 2002](#); [Mayhé-Nunes & Brandão, 2005](#); [Mayhé-Nunes & Brandão, 2007](#); [Sosa-Calvo & Schultz, 2010](#); [Ješovník et al., 2013](#); [Rabeling et al., 2015](#); [Ješovník & Schultz, 2017](#); [Sosa-Calvo et al., 2017](#); [Sosa-Calvo et al., 2018](#)). In fact an average of 2.4 new attine species have been described per year from 1995 to 2019 ([Table S1](#), e.g., [Schultz et al., 2002](#); [Ješovník et al., 2013](#); [Sánchez-Peña et al., 2017](#); [Sosa-Calvo et al., 2018](#); [Cristiano et al., 2020](#)).

Taxonomists have informally split the attines into lower and higher fungus-growing ants based on varying systems of obligate fungus-farming agriculture ([Schultz & Brady, 2008](#); [Branstetter et al., 2017](#)). The lower attines cultivate a diversity of fungal cultivar lineages, while the higher attines generally cultivate more closely related lineages of fungal species including *Leucoagaricus gongylophorus* (Möller) [Singer, 1986](#). The most derived and familiar higher attine genera consist of the leaf-cutting ants, *Atta Fabricius, 1804*, *Acromyrmex Mayr, 1865*, and *Amoimyrmex* [Cristiano et al., 2020](#) which largely cut fresh plant material for their gardens. However, the other higher attine genera consist of *Sericomyrmex Mayr, 1865*, *Trachymyrmex Forel, 1983*, *Xerolitor* [Sosa-Calvo et al., 2018](#), *Mycetomoellerius* [Solomon et al., 2019](#), and *Paratrachymyrmex* [Solomon et al., 2019](#). These non-leaf-cutting higher attines, referred to as higher attines hereafter, are phylogenetically intermediate between the lower-attine and leaf-cutting ants ([Brandão & Mayhé-Nunes, 2007](#)).

Higher attine ants share natural history traits with both the lower attines and leaf-cutting ants. Similar to leaf-cutting ants, some higher attines have also been observed cutting fresh plant material for their gardens ([Weber, 1972](#); [Schultz & Meier, 1995](#); [Leal & Oliveira, 2000](#); [Mayhé-Nunes & Brandão, 2005](#); [Brandão & Mayhé-Nunes, 2007](#)). Otherwise, much like lower attines, higher attines typically harvest fallen flowers, fruits, leaves, small twigs, seeds, and caterpillar frass ([Lizidatti, 2006](#); [De Fine Licht & Boomsma, 2010](#); [Ronque, Feitosa & Oliveira, 2019](#)). Unlike lower-attine workers that are typically monomorphic, workers in *Mycetomoellerius*, *Paratrachymyrmex*, and *Trachymyrmex* tend to be weakly polymorphic ([Weber, 1958a](#); [Beshers & Traniello, 1996](#); [Brandão & Mayhé-Nunes, 2007](#); [Rabeling et al., 2007](#)). It is this variability in worker morphology, coupled with species

descriptions based on a few workers ([Weber, 1940](#)), sampling bias (see [Mueller et al., 2018](#)), and inconsistent voucher deposition that have led to incorrect or incomplete species identifications ([Appendix Table S1](#)).

The genus *Mycetomoellerius* is represented by 31 recognized species, distributed throughout Central and South America. Taxonomic clarity for this and related genera is needed as there are likely multiple new species, including a sister clade to the well-studied species *M. zeteki* ([Weber, 1940](#); junior synonym *M. balboai*; see also [Solomon et al., 2019](#)). *Mycetomoellerius zeteki* is abundant and easily collected in the Panama Canal Zone and has been included in a large breadth of work ([Appendix Table S1](#)). Notable research includes the discovery and function of actinomycete bacteria in the fungus-growing ants ([Currie, Mueller & Malloch, 1999](#); [Mueller et al., 2008](#)), description of the evolutionary transition from single to multiple mating in the fungus-growing ants ([Villesen et al., 2002](#)), and the reciprocal evolution of ant and fungal genomes in the fungus-growing ant symbiosis ([Nygaard et al., 2016](#)). Despite this attention to its biology, *M. zeteki* has remained taxonomically ambiguous. For example, in a phylogenetic analysis of actinomycetes bacteria, three samples form a polytomy containing *M. sp. ‘Funnel’*, an undetermined *Mycetomoellerius* sp., and *M. zeteki sensu stricto* ([Cafaro & Currie, 2005](#)). It has been speculated that the current definition of *M. zeteki* may include cryptic species based on behavioral ([Adams et al., 2012b](#)), morphological ([Adams et al., 2012b](#)), molecular ([Solomon et al., 2019](#)), and chemical differences ([Adams, Jones & Jeter, 2010](#); [Adams et al., 2012a](#)).

This uncertainty surrounding *M. cf. zeteki* has ramifications given its significant historical contributions to fungus-growing ant research ([Appendix Table S1](#)). To resolve this, we use an integrative approach to clarify the taxonomy of *M. zeteki* by reexamining morphological characters, comparing old and new collections, examining morphometrics, adapting a comparative behavioral method for worker tempo, and chemically analyzing worker volatile compounds. Based on these diverse data, we recognize two species: *M. zeteki* and *Mycetomoellerius mikromelanos* sp. nov. Cardenas, Schultz, & Adams. We provide a diagnosis and description of *M. mikromelanos* sp. nov., describe the *M. zeteki* gyne wings and the morphological characters of *M. zeteki* males, determine the identity of the published *M. zeteki* genome, suggest corrections for the misidentification of voucher specimens in published research, and discuss the implications of our improved species-level definitions.

MATERIALS & METHODS

Samples and collections

Colonies of *M. mikromelanos* sp. nov. (31 colonies) and *M. zeteki* (16 colonies) were collected at the start of the wet season in 2017 and 2018 in the Canal Zone of the Republic of Panama (9.12007, -79.7317). Colony collection and fieldwork was approved by The Smithsonian Tropical Research Institute as part of the “Behavioral Ecology and Systematics of the Fungus-growing Ants and Their Symbionts (#4056)” project and the Autoridad Nacional del Ambiente y el Mar (Permiso de Colecta Científica 2017: SPO-17-173, 2018: SE/AB-1-18). Samples were collected by excavating only the first (i.e., upper) chamber of the nest to ensure colony survival. Of those excavated in 2018, 16 of 30 colonies were

collected into five-dram vials (BioQuip, Cat. 8905 California, United States) and transferred to Petri dishes lined with moist cotton fiber for observations while in Panama. Vouchers of ca. 10 or more workers and fungus gardens from each nest were collected in 95% EtOH. Live colonies were brought back to The Ohio State University to a United States Department of Agriculture Animal and Plant Health Inspection Service Approved Facility (OSU; Columbus Ohio, USA; APHIS permit P526P-16-02785; facility #4036), where they were transferred to permanent nest boxes (as in *Sosa-Calvo et al., 2015*). When colonies were excavated, many contained workers, and male and female reproductive's. We refer to the winged female reproductive caste as gynes unless otherwise noted. Few actual queens were examined. In nearly all cases, if a gyne or queen was present, there are also workers from the same colony (except one specimen from Jack Longino).

Taxonomy & morphometrics

We used a Wild M-5 microscope equipped with an ocular micrometer to examine specimens for morphological characters that unambiguously separate the two species. We also took morphological measurements of 171 workers ($n = 54$ *M. zeteki*, $n = 117$ *M. mikromelanos* sp. nov.), 53 queens and gynes ($n = 28$ *M. zeteki*, $n = 25$ *M. mikromelanos* sp. nov.), and 43 males ($n = 22$ *M. zeteki*, $n = 21$ *M. mikromelanos* sp. nov.) using standard morphometrics (Table 1). We included two synonymized *M. balboai* syntypes ('cotypes') and one additional specimen identified as *M. balboai*. Including this junior synonym of *M. zeteki* (Weber, 1958b) was necessary to confirm that *M. mikromelanos* is not *M. balboai*. Upon confirmation, these samples were included as *M. zeteki* in further analyses. Terminology for the temple and malar areas follows that of *Boudinot, Sunnicht & Adams (2013)* and for sculpturing that of *Harris (1979)*. Type and voucher specimens of material examined are deposited at the United States National Museum (USNM), Museum of Zoology of the University of São Paulo (MZSP), Smithsonian Tropical Research Institute (STRI), and The Ohio State University Museum of Biological Diversity Triplehorn Insect Collection (OSUC).

The electronic version of this article in Portable Document Format (PDF) will represent a published work according to the International Commission on Zoological Nomenclature (ICZN), and hence the new names contained in the electronic version are effectively published under that Code from the electronic edition alone. This published work and the nomenclatural acts it contains have been registered in ZooBank, the online registration system for the ICZN. The ZooBank LSIDs (Life Science Identifiers) can be resolved and the associated information viewed through any standard web browser by appending the LSID to the prefix <http://zoobank.org/>. The LSID for this publication is: urn:lsid:zoobank.org:pub:737E04E5-5A8F-48F6-BE32-ADC1028927B6. The online version of this work is archived and available from the following digital repositories: PeerJ, PubMed Central and CLOCKSS.

We partitioned specimens by caste and tested the assumption of normality for each morphometric character with a Shapiro–Wilks test. We used a Welch's *t*-test for normally distributed and a Wilcoxon Rank Sum test for non-normally distributed variables to test the null hypothesis of equal means and differences in range between both species. In

Table 1 Acronyms of standard measurements and indices used for morphology and morphometrics. Eyes are included in HW for males.

Standard measurements	
HW	Head Width, maximum width of the head, in full-face view.
HL	Head Length, maximum length diagonal from the anterior margin of the clypeus to the tip of the posterior margin of the head, in full-face view.
SL	Scape Length, the maximum length of the scape from apex to basal flange, in dorsal view. Not including the basal condyle and neck.
EL	Eye Length, maximum length of the eye, in lateral view.
FL	Frontal Lobes, maximum length from the margins of the frontal lobes, in face view.
ML	Mesosoma Length, diagonal distance from basal inflection of the anterior pronotal flange to the posterior most extension of the metapleural gland, in lateral view.
PL	Petiole Length, length from the metapleural gland to the insertion of the post-petiole, in lateral view.
PPL	Post-petiole Length, length from the anterior insertion point of the petiole to the anterior most point of the tergite-sternite gastral suture, in lateral view.
GL	Gaster Length, length from the anterior most point of the tergite-sternite gastral suture to the furthest posterior point, in lateral view.
Indices	
CI	Cephalic Index, $100 \times HW/HL$
EI	Eye Index, $100 \times EL/HL$
SI	Scape Index, $100 \times SL/HW$
FLI	Frontal Lobe Index, $100 \times FL/HW$
WaL	Waist Length, $PL + PPL$
TL	Total Length, $HL + ML + PL + PPL + GL$

the Wilcoxon Rank Sum Test there were ties in the data, so exact p -values could not be calculated for all castes. Both the normality testing and difference of means was performed in the base R package ‘stats’ ([R Core Team, 2017](#)). To reduce the risk of Type I error, only measurements with a Bonferroni corrected P -value ($p < 0.003$) were included.

With our retained variables, we performed non-metric multidimensional scaling (NMDS) with the vegan R package, using the ‘metaMDS’ function ([Oksanen et al., 2019](#)). This function calculates the Bray-Curtis distances, applies a square root transformation, and scales the distance measures down to k dimensions. We set $k = 2$ and searched for a solution with 1,000 random starts (see [McCune & Grace, 2002](#); [Glon et al., 2019](#); [Oksanen et al., 2019](#)). We subsequently produced a diagnostic Shepard plot with the ‘stressplot’ command from vegan. We considered our reduced dimensions acceptable if our transformed data reasonably fit the regression of the Shepard plot and if stress scores were < 0.20 ([McCune & Grace, 2002](#)). We generated NMDS plots with characters plotted as vectors and 95% confidence ellipses for each species.

Behavioral assay

We adapted the novel environment assay ([Chapman et al., 2011](#)) to examine the tempo, i.e., activity level, of workers of *M. zeteki* and *M. mikromelanos* sp. nov. We subsampled four colonies of each species with five trials per colony. Single workers were selected from the foraging chamber and placed in the center of a nine cm Petri dish lined with one

cm² grid paper. The ant was immediately covered with one quarter of a 4.5 cm weigh boat (referred to as “refuge” hereafter). Five-minute trials were recorded with a Sony DCR-PC109 camera, digitized from the cassette tape, and scored using Solomon Coder ([Péter, 2017](#)). We measured (1) time to initially emerge from the refuge, (2) number of squares the ant entered, and (3) time spent under the refuge after the initial emergence. To analyze the change in tempo over the trial, we produced a ratio of squares entered to time spent entering squares (i.e., not under the refuge): New Squares/(300 s - Time to Exit Refuge - Time Under Refuge - Time on Refuge) = Tempo.

To test whether tempo differed between species we used a generalized linear mixed model (GLMM) with the ‘lme4’ package ([Bates et al., 2015](#)) in R ([R CoreTeam, 2017](#)). This experiment included multiple workers from the same colony, which are not independent from one another. To account for the blocked design (i.e., multiple data points from the same colony), we included the workers’ colony of origin as a random effect in the model. We compared a linear mixed model and multiple GLMMs using gaussian and gamma distribution families with the log, identity, and inverse link functions. To confirm the fit of the model, we first checked the normality of the residuals using a QQ-plot and Shapiro–Wilk test. We then checked for linearity and homoscedasticity by plotting the residuals and fitted values.

Phylogenetic analysis

We used sequence data published in [Solomon et al. \(2019\)](#); available on Dryad DOI: [10.5061/dryad.2p7r771](https://doi.org/10.5061/dryad.2p7r771)) to confirm the identity of the published genome ([Nygaard et al., 2016](#)). We used sequences of *M. zeteki*, *M. mikromelanos* sp. nov. (listed as *Mycetomoellerius* n. sp. RMMA in [Solomon et al., 2019](#); [Table S2](#)), and *M. turrifex* ([Wheeler, 1903](#)) from the dataset of [Solomon et al. \(2019\)](#) and aligned them in Geneious (version R9; Biomatters Limited, Auckland, New Zealand). We used BLAST with blastn and megablast ([Altschul et al., 1990](#); [Zhang et al., 2000](#); [Morgulis et al., 2008](#)) to identify quality gene regions in the published genome ([Nygaard et al., 2016](#); GenBank accession: [GCA_001594055.1](https://www.ncbi.nlm.nih.gov/nuccore/GCA_001594055.1)). The gene for COI was removed from the analysis because COI data were missing for a subset of individuals in the data of [Solomon et al. \(2019\)](#). Megablast found no alignments and blastn found multiple scaffolds with high query cover (see Results and [Table S3](#)). In Geneious, we mapped our samples to the identified reference genome scaffolds and trimmed the areas of the scaffold that did not align. Once aligned, we concatenated our data into a multi-locus dataset with SequenceMatrix 1.8 ([Vaidya, Lohman & Meier, 2011](#)) for phylogenetic analysis. The four genes used are elongation factor 1-alpha F1 (*EF1α*-F1 1,074 bp), elongation factor 1-alpha F2 (*EF1α*-F2 434 bp), long-wavelength rhodopsin (*LwRh* 455 bp), and wingless (*WG* 702 bp).

For our phylogenetic analysis, we used ModelFinder ([Kalyaanamoorthy et al., 2017](#)) in IQ-TREE (version 1.6.10; [Nguyen et al., 2015](#)) to determine the best evolutionary model for each gene. The partitions with the most similar and likely models were merged in IQ-TREE and used to construct a maximum-likelihood phylogeny with *M. turrifex* as the outgroup and 10,000 ultrafast bootstraps (UFboot2; [Hoang et al., 2018](#)). Our resulting consensus tree was annotated in FigTree (version 1.4.3; [Rambaut, 2016](#)) and edited in Adobe Illustrator.

Chemical analysis

Volatile compounds were extracted from workers (as in [Hamilton et al., 2018](#)) sampled from lab-maintained colonies of *M. mikromelanos* sp. nov. ($n = 6$ colonies) and *M. zeteki* ($n = 4$ colonies). Samples of 4–10 individuals per colony were placed in HPLC grade methanol solvent. Whole ants from the same colony, or trisected ants (head, thorax, gaster), were placed in separate glass vials with 40–100 μL of solvent. Trisections were used to identify where the most abundant compounds were found and whole specimen extractions confirmed the presence of the compounds. Tools used for trisections were rinsed with ethanol, methanol, and pentane between trisection to prevent cross-contamination. Samples were stored at -20°C until analysis by gas-chromatography mass-spectrometry (GC-MS). Reported compounds were found in at least trace amounts in two or more extracts of workers of the same species.

Samples of extracts were analyzed at the Virginia Military Institute with gas chromatography–mass spectrometry (GC-MS; as in [Hamilton et al., 2018](#)) using a Shimadzu QP-2010 GC-MS equipped with an RTX-5, 30 m \times 0.25 mm i.d. column. The carrier gas was helium with a constant flow of 1 ml/min. The temperature program was from 60 to 250 $^\circ\text{C}$ changing 10 $^\circ\text{C}/\text{min}$ and held at the upper temperature for 20 min. The mass spectrometer was operated in EI mode at 70 eV, and scanning was set to 40 to 450 AMU at 1.5 scans/s. Peaks on chromatograms were identified by database search (NIST Mass Spectral Data base, V.2, US Department of Commerce, Gaithersburg, MD), published literature spectra, and by direct comparison with commercially available authentic samples. We standardized our resulting compounds for comparison. For each sample, ratios from the chromatogram peaks were converted to proportions and visualized in Adobe Illustrator.

Literature review

We conducted a literature review for all papers referencing *M. zeteki* or *M. cf. zeteki* to identify potentially misnamed species. Using the research databases Web of Knowledge (Clarivate Analytics, Massachusetts, United States), antweb.org (California Academy of Sciences, California, United States), hol.osu.edu (C.A. Triplehorn Insect Collection, Ohio, United States), and personal literature collections, we reviewed papers that were found by the search criterion “*Trachymyrmex zeteki*”, “*Trachymyrmex cf. zeteki*”, “*T. zeteki*”, “*T. cf. zeteki*”, “*zeteki*”, and “*cf. zeteki*”. We then selected articles that included *M. cf. zeteki* or *M. zeteki* as their focal research organism and recorded those that reported the deposition of voucher specimens. We disregarded research articles that did not use physical specimens (e.g., data from molecular databases).

RESULTS

Morphometrics

Nearly all measurement means (Welch's), and ranges (Wilcoxon) are different between the two species ([Table 2](#)). The samples of the junior synonym *M. balboai* are within the ranges of *M. zeteki* samples (see [Table S4](#)) and are morphologically similar to the *M. zeteki* type specimen. *M. mikromelanos* sp. nov. is on average smaller than *M. zeteki* except in the case

of the frontal lobe index (FLI). Due to non-significant differences, FLI was excluded from analyses of males and gynes. We observed some overlap in the range of measurements for workers and for males between *M. mikromelanos* sp. nov. and *M. zeteki*. In contrast, gynes are very distinct with few overlapping ranges (Table 2).

WORKERS: For our worker partition, all 15 characters were significantly different between species ($p < 0.003$; Table 2). Our NMDS converged on a two-dimensional solution with an acceptable stress level (stress = 0.1288) and the Sheppard plot showed good association around the regression line (non-metric fit $R^2 = 0.983$; linear fit $R^2 = 0.933$; see Fig. S1a). The resulting NMDS plot shows some overlap between the ellipses, although each species forms a distinct cluster with few outliers (Fig. 1A). The vectors for head width (HW), scape index (SI), and petiole length (PL) showed the most strength and direction in the measurements relative to the NMDS axes (Fig. 1A). Additionally, the type specimens for *M. mikromelanos* sp. nov. and *M. zeteki* plotted within their own ellipses (Fig. 1A). While the *M. mikromelanos* sp. nov. type and paratype specimens fall within the overlap of ellipses for both species, they remain morphologically distinct (see diagnosis and description). For *M. mikromelanos* sp. nov., SI and FLI explain separation from the *M. zeteki* cluster; while HW, eye length (EL), and frontal lobe FLI explain separation from *M. mikromelanos* sp. nov. for *M. zeteki*. However, PL and waist length (WaL) best explain variation within clusters along the Y axis. Lastly, the two synonymized *M. balboai* syntype ('cotype') samples fall well within the *M. zeteki* ellipses.

GYNES: For the gyne partition, all but FLI ($p = 0.6110$) were significantly different between species ($p < 0.003$; Table 2). The NMDS converged on a two-dimensional solution with a robust stress level (stress = 0.1119), and the Sheppard plot showed a strong association around the regression line with a single outlier (non-metric fit $R^2 = 0.986$; linear fit $R^2 = 0.941$; see Fig. S1b). The NMDS plot showed *M. mikromelanos* sp. nov. and *M. zeteki* each forming distinct clusters with two outliers (Fig. 1B). The *M. mikromelanos* sp. nov. paratype gyne fell well within the *M. mikromelanos* sp. nov. cluster (Fig. 1B). The vectors EL, SI, and PL showed the most strength in directionality of the measurements relative to the NMDS axes (Fig. 1B).

MALES: For our male partition, all but FLI ($p = 0.0307$) were significantly different between species (Table 2). The NMDS converged on a two-dimensional solution with a robust stress level (stress = 0.1554). The Sheppard plot also showed relatively high correlation with the regression line (non-metric fit $R^2 = 0.976$; linear fit $R^2 = 0.886$; see Fig. S1c). The NMDS plot showed *M. mikromelanos* sp. nov. and *M. zeteki* each forming distinct clusters with no outliers. The vectors for PL, mesosoma length (ML), SL, and cephalic index (CI) show the most strength in directionality of the measurements relative to the NMDS axes (Fig. 1C). The paratypes for both males fell well within their species clusters.

Our morphometric analysis shows that *M. mikromelanos* sp. nov. and *M. zeteki* are distinct species while supporting the previous synonymy of *M. balboai* under *M. zeteki* by Weber (1958b). Nearly all of the measurements taken are significantly different for all castes. The NMDS plots reflect the overlap of some measurements observed in workers and males while depicting clear separation of measurements observed in gynes.

Table 2 Select morphometrics of all castes. Partitioned mean values, standard errors (SE), minimum and maximum standard measurements in millimeters, except indices (see Table 1) for workers, gynes, and males (cont'd) of *M. mikromelanos* sp. nov. and *M. zeteki*. Presented morphometrics were chosen based on vectors from NMDS plots with the most directionality (see Fig. 1A). All samples except for singleton workers of *M. mikromelanos* worker (Panama, Darién Provence) and gyne (Costa Rica, Heredia Provence) are from the Panama Canal Zone.

	Mean	SE	Min	Max
<i>M. mikromelanos</i> sp. nov. workers				
<i>N</i> = 117 (28 nests)				
HW	1.123	0.004	1.012	1.215
EL	0.201	0.001	0.165	0.230
ML	1.657	0.007	1.441	1.911
PL	0.409	0.004	0.310	0.507
CI	114.007	0.339	102.761	123.517
SI	91.829	0.226	87.792	100.194
TL	4.402	0.017	3.843	4.877
<i>M. zeteki</i> workers				
<i>N</i> = 54 (13 nests)				
HW	1.435	0.013	1.208	1.602
EL	0.256	0.002	0.207	0.286
ML	1.972	0.018	1.665	2.248
PL	0.482	0.007	0.385	0.605
CI	122.141	0.390	115.790	127.767
SI	81.329	0.311	77.441	86.661
TL	5.181	0.046	4.520	6.043
<i>M. mikromelanos</i> sp. nov. gynes				
<i>N</i> = 25 (9 nests)				
HW	1.298	0.005	1.267	1.380
EL	0.270	0.004	0.231	0.304
ML	2.028	0.008	1.915	2.112
PL	0.599	0.010	0.507	0.704
CI	113.715	0.535	104.546	119.481
SI	79.847	0.405	73.478	84.451
TL	5.659	0.018	5.435	5.814
<i>M. zeteki</i> gynes				
<i>N</i> = 28 (10 nests)				
HW	1.652	0.011	1.462	1.800
EL	0.378	0.003	0.333	0.399
ML	2.478	0.012	2.272	2.584
PL	0.756	0.016	0.539	0.873
CI	119.933	0.423	115.980	126.677
SI	73.602	0.255	71.111	75.923
TL	6.965	0.043	6.072	7.296
<i>M. mikromelanos</i> sp. nov. males				
<i>N</i> = 21 (5 nests)				
HW	0.840	0.004	0.817	0.893
EL	0.294	0.003	0.282	0.310

(continued on next page)

Table 2 (continued)

	Mean	SE	Min	Max
ML	1.781	0.012	1.671	1.859
PL	0.369	0.006	0.338	0.437
CI	122.934	0.956	115.437	134.084
SI	98.407	0.618	91.713	103.427
TL	4.550	0.035	4.196	4.759
<i>M. zeteki</i> males				
N = 22 (6 nests)				
HW	1.043	0.009	0.957	1.140
EL	0.368	0.003	0.338	0.399
ML	2.015	0.020	1.830	2.168
PL	0.500	0.010	0.422	0.591
CI	130.871	1.012	125.826	142.322
SI	96.988	0.822	86.822	102.687
TL	5.334	0.059	4.984	5.902

Behavioral assay

The tempo of worker activity differed between the two species (Fig. 1D). A gamma distribution with an inverse link function was the best fit model (Table 3). For our diagnostic analysis of our GLMM see supplementary material (Figs. S2–S4). The gamma inverse model shows that tempo was correlated with species (Table 3, $\text{Pr}(>|z|) = 1.150 \times 10^{-2}$) and the variance of the random effect (colony) was not significant ($\text{var.} = 7.977 \times 10^{-2}$). This indicates that the variation observed in tempo was associated with species identity rather than with the particular colony of origin. This result provides further support for the delimitation between *M. zeteki* and *M. mikromelanos* sp. nov.

Phylogenetic analysis

Using published data (Nygaard *et al.*, 2016; Solomon *et al.*, 2019) located in GenBank (*Mycetomoellerius zeteki* genome: GCA_001594055.1) and the *Mycetomoellerius* gene sequences (Dryad DOI: 10.5061/dryad.2p7r771; GenBank accession numbers Table S2) we found genetic differences between *M. mikromelanos* sp. nov. and *M. zeteki*, with the former supported as genetically distinct from the latter by 100% bootstrap support (Fig. 1E). We located scaffolds for four genes (i.e., *EF1α-F1*, *EF1α-F2*, *LwRh*, and *WG*) and found high support for each in the published genome. For the mitochondrial gene *COI*, commonly used for DNA barcoding (Simon *et al.*, 1994), 12 scaffolds were identified in the *M. zeteki* genome and only five had >95% query cover (Table S3) suggesting the presence of pseudogenes and rendering this marker unreliable (Leite, 2012). Based on the BIC scores, ModelFinder joined *EF1α-F1* + *WG* (62 unique and 19 informative of 1777 sites) and *EF1α-F2* + *LwRh* (13 unique and 6 informative of 972 sites) partitions and found the K2P+I and K2P to be the best fit models for those partitions respectively. The samples RMMA090930-09, RMMA050105-29, JSC030826-01, and the genomic scaffold sequences used (GCA_001594055.1) were identified as identical. Our phylogenetic analysis using four genes provided strong support for identifying the Nygaard *et al.* (2016) genome as belonging to *M. mikromelanos* sp. nov. rather than to *M. zeteki* as reported.

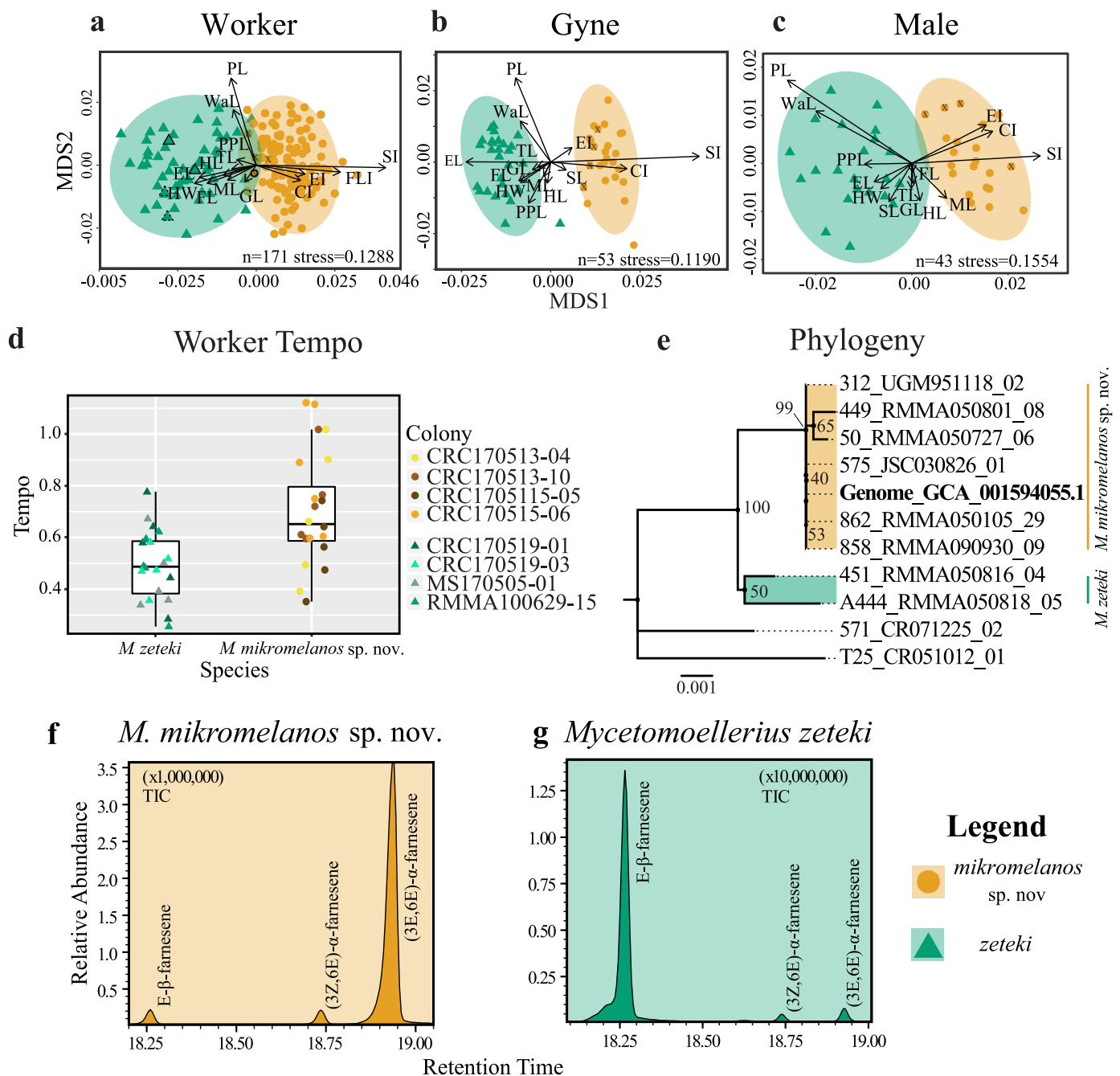


Figure 1 Integrative taxonomy results. Non-metric multidimensional scaling (NMDS) plots of worker (A), gyne or queen (B) and male (C) morphology. HW = head width, HL = head length, SL = scape length, EL = eye length; FL = frontal lobes, ML = mesosoma length, PL = petiole length, PPL = post-petiole length, GL = gaster length, CI = cephalic index, EI = eye index, SI = scape index, FLI = frontal lobe index, WI = waist length, TL = total length. SL is removed from worker NMDS (A) given its short vector and to show the *M. mikromelanos* sp. nov. type. Type specimen are indicated by a solid bold outline for both species, where the synonymized *M. balboai* (now *M. zeteki*; Weber 1958) is indicated with a dashed line, and paratypes are indicated by X's. (D) Worker tempo differences between *M. zeteki* and *M. mikromelanos* sp. nov.. (E) Reconstructed multi-locus phylogeny indicates that the published genome from (Nygaard et al., 2016; GCA_001594055.1) belongs to the new species, *M. mikromelanos* sp. nov.. Chemical chromatograms of *M. mikromelanos* sp. nov. (F) and *M. zeteki* (G) worker gasters indicating abundance differences of farnesenes: (1) E- β -farnesene, (2) (3Z,6E)- α -farnesene, (3) (3E,6E)- α -farnesene; with *M. mikromelanos* sp. nov. having a high abundance of (3) and low abundances (1) and (2), and *M. zeteki* having high abundance of (1) and low abundance of (2) and (3).

Full-size DOI: 10.7717/peerj.11622/fig-1

Table 3 Tempo analysis results. Generalized linear mixed-effects models tested and compared. Each model had 40 observations, 20 each for *M. mikromelanos* sp. nov. and *M. zeteki*. Species and constant rows are the fixed effects estimates. Values in parentheses are standard errors (SE) for the cell above. The Gamma Inverse model was the best-fit model based on all diagnostics measures.

Fixed effects	Linear mixed model	Gaussian Log-Link	Gamma Log-Link	Gamma identity	Gamma inverse
Species (SE)	-0.593*** (0.161)	0.348*** (0.116)	0.343** (0.101)	0.203*** (0.055)	-0.589*** (0.181)
Constant (SE)	2.031*** (0.132)	-0.712*** (0.090)	-0.709*** (0.072)	0.492*** (0.032)	2.035 *** (0.143)
Log Likelihood	8.887	12.889	14.765	14.711	14.848
Akaike Inf. Criterion	-9.739	-17.778	-21.530	-21.422	-21.695
Bayesian Inf. Criterion	-2.983	-11.023	-14.774	-14.667	-14.940

Notes.

*** $p < 0.01$.

Table 4 Volatile worker compounds. The average relative amount of six *M. mikromelanos* sp. nov. and four *M. zeteki* colonies sampled and standard error for compounds found in workers of both species. Worker farnesenes **Farn. 1**: E- β -farnesene, **Farn. 2**: (3Z,6E)- α -farnesene, and **Farn. 3**: (3E,6E)- α -farnesene.

Compound		Farn. 1	Farn. 2	Farn. 3
Retention time		18.27	18.74	18.93
<i>mikromelanos</i> sp. nov.	6	0.133 ±0.08	0.089 ±0.04	0.693 ±0.13
<i>zeteki</i>	4	0.622 ±0.14	0.184 ±0.10	0.065 ±0.01

Chemical analysis

We found three farnesene compounds in *M. mikromelanos* sp. nov. and *M. zeteki* workers (1) E- β -farnesene, (2) (3Z,6E)- α -farnesene, and (3) (3E,6E)- α -farnesene, in whole samples and gaster trisections. Farnesenes have been reported before and are presumably localized in the gaster, functioning as trail pheromones (Adams et al., 2012a; Figs. 1F & 1G; Table 4). (3E,6E)- α -farnesene (3) is most abundant in *M. mikromelanos*, averaging 69.3% of the observed farnesenes. (1) and (2), are each at less than 23% of the overall abundance in *M. mikromelanos* sp. nov. E- β -farnesene (1), is the most abundant (62.2%) in *M. zeteki* with (2) at 18.4% and (3–5) with 6.5%.

These results illustrate that unique worker chemical profiles distinguish the two species. Some samples contained dilute concentrations of compounds as seen by the relative abundance (Figs. 1F & 1G). One *M. mikromelanos* sp. nov. colony (CRC170518-08) has a chemical profile similar to *M. zeteki*, with (1) 56.9%, (2) 33.7%, and (3) 9.3%. While this one colony stands out, all of the colonies of *M. mikromelanos* sp. nov. analyzed are morphologically distinct from *M. zeteki* and fit the description of *M. mikromelanos* (see Taxonomy section).

Literature review

We found 63 articles that used *M. zeteki* or *M. cf. zeteki* under our search criteria (see Appendix Table S1). Twenty-eight articles did not identify the repositories of their voucher

specimens, and of these, three articles deposited online sequence vouchers for ant specimens but mentioned no corresponding voucher specimens; nine others deposited symbiont vouchers (two fungal cultivar and seven non-cultivar symbionts). Voucher specimens were deposited in museums around the globe ([Appendix Table S1](#)), with the greatest number (fifteen) deposited at the Smithsonian Institution National Museum of Natural History, United States (USNM). The full list of voucher repositories includes: Colección Nacional de Referencia Museo de Invertebrados Universidad de Panamá (Panama); Smithsonian Tropical Research Institute Panama (Panama); Museu de Zoologia da Universidade de São Paulo (Brazil); Instituto Nacional de Biodiversidad (Costa Rica); Museo de Entomología de la Universidad del Valle (Colombia); Museo Entomológico Universidad Nacional Agronomía Bogotá (Colombia); Museum at the Universidad Técnica Particular de Loja (Ecuador); Natural History Museum of Denmark, (Denmark); Zoological Museum of the University of Copenhagen (Denmark); Zoological Museum, University of Puerto Rico (Puerto Rico); and the Smithsonian Institution National Museum of Natural History, (United States of America).

***Mycetomoellerius mikromelanos* sp. nov.** Cardenas, Schultz, & Adams, new species
[Figs. 2](#) and [3](#) include *M. mikromelanos*.

Geographic range: Panama: Colón, Darién, and Panama Province (RMMA and Jack Longino (JTL) specimens).

Label text: Separate labels for each specimen indicated by brackets (e.g., [Label 1] [Label 2]).

HOLOTYPE: Worker, Republic of Panama. [9.16328, -79.74413, Panama: Colón Province, Pipeline Rd, 16E, 62m, 13.v.2017, Cody Raul Cardenas, CRC170513-04] [USNMENT01123723]. Repository: USNM.

PARATYPES: 15 Workers, Republic of Panama. Same label data as holotype. Repositories: USNM (3): USNMENT01123726, USNMENT01123727, USNMENT01123728; MZSP (4): OSUC 640618, OSUC 640619, OSUC 640620, OSUC 640621; STRI (5): OSUC 640635, OSUC 640636, OSUC 640637, OSUC 640638, OSUC 640639; OSUC (3): OSUC 640606, OSUC 640607, OSUC 640608.

PARATYPES: 11 Gynes, Republic of Panama. Same label data as holotype. Repositories: USNM (4): USNMENT01123724, USNMENT01123729, USNMENT01123730, USNMENT01123731; MZSP (3): OSUC 640622, OSUC 640623, OSUC 640624; STRI (3): OSUC 640640, OSUC 640641, OSUC 640642; OSUC (1): OSUC 640609.

PARATYPES: 7 Males, Republic of Panama. Same label data as holotype. Repositories: USNM (4): USNMENT01123725, USNMENT01123732, USNMENT01129733, USNMENT01129734; MZSP (1): OSUC 640625; STRI (1): OSUC 640643; OSUC (1): OSUC 640610.



Figure 2 *Mycetomoellerius mikromelanos* sp. nov. type (A–C) and gyne paratype (D–F) specimens. (A) Worker profile. (B) Worker head full-face view; FL = Frontal Lobe spine; CE = Compound Eye; Dsc = Head capsule Disc; Scp = Scape. (C) Dorsal worker view. (D) gyne paratype full-face view; AR = Arcuate Ridge; OS = Occipital Spine; Oc = Ocelli. (E) Gyne lateral view, Ha = Hamuli. (F) Gyne dorsal view Sclp = sculpturing.

Full-size DOI: 10.7717/peerj.11622/fig-2

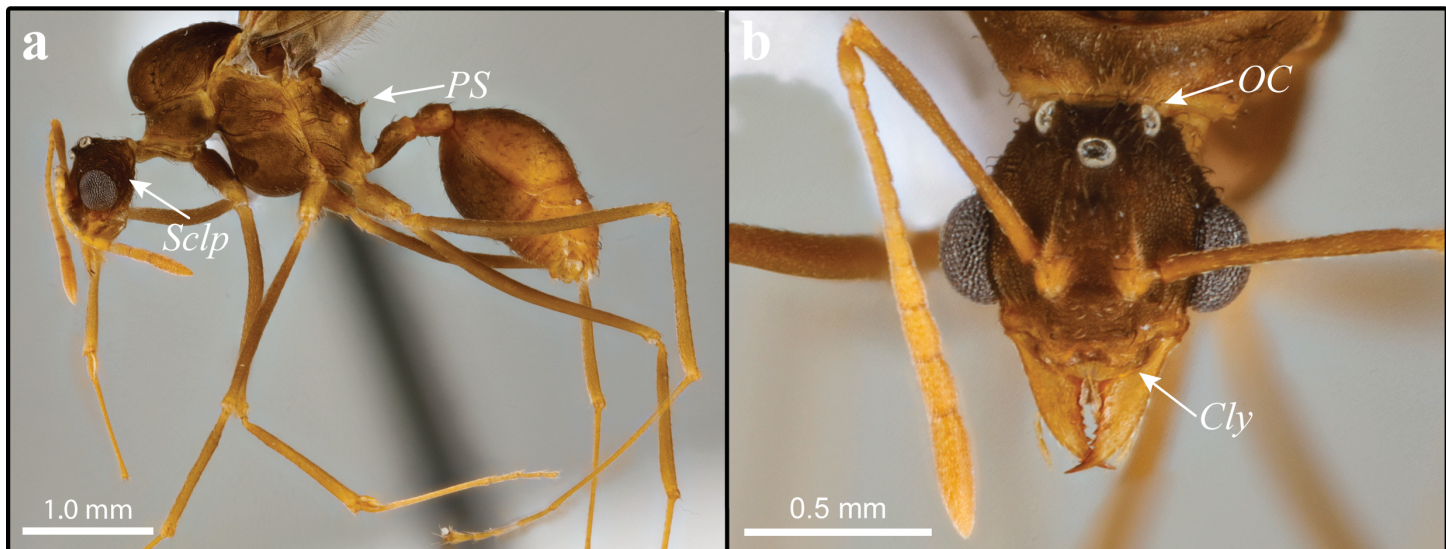


Figure 3 *Mycetomoellerius mikromelanos* sp. n. male paratype specimen. (A) profile, lateral view, *Sclp* = Sculpturing; *PS* = Propodeal Spine. (B) head full-face view *Cly* = Clypeus impression corners; *OC* = Oceli.

[Full-size](#) DOI: 10.7717/peerj.11622/fig-3

HOLOTYPE/PARATYPE Colony Code: CRC170513-04.

Additional material examined:

Workers N = 12: USNM: 3 specimens sharing label data [PANAMA: Pipeline RD, La Seda River; 79.736°W 9.1529°N; 28 v 2010;] [Henrik H. De Fine Licht; nest series; river bank; underground' HDFL28052010-4 ch1][*Trachymyrmex zeteki*] [Check cryo] [DO NOT REMOVE SI DB Reference Not a property tag T. Schultz, NMNH] USNMENT00752565, USNMENT00752578, USNMENT00752579; 4 specimens sharing label data [PANAMA: Pipeline Rd, La Seda River; 79.736°W, 9.1529°N; 28 v 2010;] [Henrik H. De Fine Licht nest series; river bank; underground HDFL28052010-5] [*Trachymyrmex zeteki*] [See cryo collections] [DO NOT REMOVE SI DB Reference Not a property tag T. Schultz, NMNH]: USNMENT00752574, USNMENT00752580, USNMENT00752581, USNMENT00752582; 3 specimens sharing label data [PANAMA: Pipeline Road, 2km past Limbo River 12v2010] [Henrik H. De Fine Licht; nest series; river bank; underground HDFL120502010-14] [*Trachymyrmex zeteki*] [See also cryo collections] [DO NOT REMOVE SI DB Reference Not a property tag T. Schultz, NMNH]: USNMENT00752565, USNMENT00752578 (1 pin with 2 specimens), USNMENT00752579. JTL: 1 specimen [PANAMA, Darién: 5 km S Platanilla 8.78105 -78.-41251 ±20 m 160 m, 20an2015 J. Longino#9082] [2nd growth veg. stream edge nest in clay bank] [CASENT0633645].

Males N = 3: USNM: 3 specimens sharing label data [PANAMA: Pipeline Road, 2km past Limbo River 12v2010] [Henrik H. De Fine Licht; nest series; riverbank; underground HDFL120502010-14] [*Trachymyrmex zeteki*] [See also cryo collections] [DO NOT REMOVE SI DB Reference Not a property tag T. Schultz, NMNH] USNMENT00752576, USNMENT00752578 (1 pin with 2 specimens).

Note: A name previously applied to this species, *Trachymyrmex fovater*, was incorrectly electronically published in a conference poster format and is therefore unavailable ([Cardenas et al., 2016](#)). This name is unavailable because (i) the date of the publication was not indicated on the poster and (ii) the name was not registered in the Official Register of Zoological Nomenclature ([ICZN, 1999](#)). We hereby describe *Mycetomoellerius mikromelanos* sp. nov. (LSID: urn:lsid:zoobank.org:act:B6BABA13-708F-44D8-AD2C-F4D5B8FB03E8), a name more appropriate for this species (see Etymology) and provide a complete diagnosis and description of this new species.

Diagnosis: Measurements for all castes are in [Table 2](#) and [Table S4](#). We found characters that reliably separate *M. mikromelanos* sp. nov. from *M. zeteki*. However, due to the variability of worker castes (e.g., mesosoma spines), intermediate character states occur in some individuals. The following characters are those most useful for diagnosis.

Workers (1) cuticle coloration dark-ferruginous ([Figs. 2A–2C](#)); (2) overall integument bearing granulose irrorate sculpturing ([Figs. 2A–2C](#)); (3) frontal lobe with crenate margins and weak antero-lateral spine ([Fig. 2B](#)); (4) hooked spatulate bi-colored setae medial to frontal carina on disc of head capsule ([Fig. 2B](#)); (5) scape surpassing occipital corners when lodged in antennal scrobe ([Fig. 2B](#)); (6) convex margin of the compound eye extending past the lateral border of the head by more than half of its visible diameter in full-face view ([Fig. 2B](#)).

Gynes (1) cuticle coloration dark-ferruginous ([Figs. 2D–2F](#)); (2) supraocular spine superior to compound eye by more than or equal to the eye length ([Fig. 2D](#)); (3) small arcuate ridge superior to and reaching anterior ocellus, with its terminal ends directed postero-laterally ([Fig. 2D](#)); (4) lateral ocelli partially obscured in full-face view ([Fig. 2D](#)); (5) mesoscutum with random-reticulate sculpturing ([Fig. 2F & S5a](#)); (6) wings bicolored, venation ferruginous-brown ([Figs. 2E, 2F\] & S5b](#)); (7) hindwing with 7–9 hamuli ([Fig. 2E & S5b](#)).

Males (1) bicolored; head and mesosoma ferruginous-brown; metasoma dark testaceous-orange ([Fig. 3A](#)); (2) complete carinate-rugulose sculpturing of posterior head capsule, arranged nearly perpendicular to the longitudinal axis of the head ([Fig. 3A](#)); inferior to frontal lobe, sculpturing sparsely carinate and finely reticulate ([Fig. 3A & S6](#)); (3) mandible distinctly smaller compared to *M. zeteki*; (4) corners of medial clypeal emargination rounded ([Fig. 3B & S6](#)) ocelli smaller relative to *M. zeteki* in full-face view, occipital corner of head capsule visible ([Fig. 3B](#)); (6) propodeal spines wider at base than long ([Fig. 3A](#)).

WORKER: Overall pilosity is strongly bicolored, terminating with light coloration when spatulate; unless otherwise noted curved, appressed, and simple ([Figs. 2A–2C](#)). Older workers dark-ferruginous; younger workers ferruginous-orange. Integument typically with granulose irrorate sculpturing and a variably present white cuticular bacterial bloom.

Head: Disc of head capsule bears spatulate bi-colored setae ([Fig. 2B](#)); weakly granulose sculpturing; in full-face view broader than long. Mandible feebly sinuous, with 6–9 denticles. Palpal formula 4,2. Median margin of clypeus impressed; lateral-most corners of impression distinctly angulate. Preocular carina originate from mandibular insertion and terminate at occipital corners by a stout multituberculate tumulus directed postero-laterally. Frons with simple bi-colored setae. Frontal lobe semicircular; crenate margins

and weak antero-lateral spine (Fig. 2B); frontal carina extending from posterior margins reaching occipital corners, joining the sub-parallel preocular carina to form antennal scrobes. Eye with 6-7 facets across width; eye margin extending past the lateral border of the head by more than half of its visible diameter in full-face view (Fig. 2B). Antenna with 11 segments; when lodged in antennal scrobe scape surpasses occipital corner (Fig. 2B); scape wide proximally and weakly tapering before thickening sub-distally; scape narrow at apex. Supraocular projection stout and multituberculate. Vertex impression shallow and narrow, but variable.

Mesosoma: Erect and strongly curved spatulate setae typically occurring from, or near, tubercles or spines; sparse rugulose sculpturing; most mesosomal sclerites with fine granulate sculpturing. Pronotum with fused median pronotal tubercles; superior lateral pronotal spine project antero-laterally; inferior lateral pronotal spines that project anteroventrally; in most cases the median pronotal spine projects as far or farther than lateral pronotal spine. Coxa I with entirely simple weakly bicolored setae; subtle superior impression on its anterior margin. Coxae II and III have spatulate setae on parallel carina dorso-laterally. Legs with spatulate setae proximally gradually becoming simple, appressed, and pale distally. Propodeum, in lateral view presents tuberculate carina at anterior base of propodeal spine; superior margin of metapleural gland bulla with variable number of tubercles; carina occurring from spiracle to propodeal lobes.

Metasoma: Petiolar nodes granulate and present a variable number of spines. Petiole with spatulate seta medially and posteriorly; intermittent carina comprised of tubercles; carina turn weakly mesad anteriorly but do not touch each other; lateral posterior margin weakly convex; in dorsal view anterior margins rounded (Fig. 2C); in dorsal view lateral margins subtly crenulate and weakly concave sub-anteriorally; ventral carinae converges to sub-petiolar process. Postpetiole with spatulate setae scattered dorsally and laterally; pair of simple setae ventrally; dorsal carina comprised of tubercles; in dorsal view, broader than long dorsally; posterior margin flat medially, with medial impressions on lateral margins. Gaster tergites and sternites with spatulate setae anteriorly; posterior margin of first tergite with subtly curved, simple setae; all other tergites and sternites with simple setae that become gradually finer and lighter posteriorly; weak reticulate sculpturing; triangular; in lateral view mostly round; first gastral tergite has crenate postero-lateral corners that surpass thin shiny margin between tergites I and II.

GYNE: Dark, curved, and simple setae unless otherwise noted; queens uniform ferruginous-orange color; increasingly dark-ferruginous with age. Integument generally with irrorate sculpturing and a variably present white cuticular bacterial bloom (Figs. 2D–2F).

Head: Setae of head capsule dark, curved, appressed, and simple; disc of head capsule bearing some spatulate setae; prominent sculpturing throughout; in full-face view, head longer than broad. Mandible feebly sinuous, with 6–8 denticles. Clypeus with minute tubercles scattered from anterior margin to slightly anterior of frontal lobes. Frontal lobe disc weakly rugulose; antero-lateral margin with reduced spine; semicircular; carina interior and parallel to margins. In full-face view, at least three quarters of the anterior lateral margin of compound eye surpassing lateral margin of head capsule; supraocular

spine separated from compound eye by as much or more than the eye length (Fig. 2D; i.e., EL = 0.27 mm, distance to supraocular spine = 0.31 mm). Antennal scape wide proximally and tapering slightly before thickening sub-distally. Vertex carina extending from ocelli to frontal carinae; small arcuate ridge touches posterior margin of ocellus superior to anterior ocellus with terminal ends directed variably laterally and posteriorly but never anteriorly. Vertex variably impressed, but generally shallow and narrow.

Mesosoma: Sclerites with spatulate setae; confused-rugulose sculpturing. Pronotum with stout medial spine projecting anteriorly; superior lateral pronotal spine projecting antero-laterally; inferior lateral pronotal spine flattened laterally and projecting ventro-laterally. Coxa I with dark curved anterior setae and minute dense lightly colored pilosity throughout; weak asperous sculpturing on lateral face. Coxa II with bicolored weakly to fully spatulate setae along parallel carinae; a row of thick, dark, curved setae on posterior side in lateral view; rugulose sculpturing lateral to carinae. Coxa III has bicolored weakly to fully spatulate setae along carinae otherwise simple setae throughout; rugulose sculpturing lateral to carinae. Mesoscutum with appressed weakly spatulate to simple bicolored setae; random reticulate sculpturing. Mesoscutellar disc with appressed setae; random reticulate sculpturing (Fig. 2F & S5a); two small posteriorly projecting spines. Axilla hides scutoscutellar sulcus. Katepisternum and anepisternum suture embossed with strigate sculpturing. Inferior margin of anepisternum crenulate. Propodeal declivity nearly vertical.

Wings: Wings with a fine pubescence. Tegula with fine curved setae; triangular; weakly impressed on its face. Axillary sclerite with fine curved setae; flattened along distal margin. Forewing tinted smokey gray, more so anteriorly and less so posteriorly; venation ferruginous-brown; with five cells (Fig. 2F & S5b); length of radial sector-media greater than half the length of the radius radial sector (Fig. S5b). Hindwing with long fine setae on posterior margin, longer proximally than distally; tinted smokey gray, more so anteriorly and less so posteriorly; venation ferruginous-brown; two cells; 7–9 hamuli (Figs. 2D, 2F & S5b).

Metasoma: Petiole with weakly curved and bicolored setae, variably spatulate to simple; dorsal carinae of petiole with parallel spines that touch posterior margins; dorsal carinae directed medioanteriorly but not joining; ventral carinulae converging posteriorly on sub-petiolar process. Post-petiolar dorsum with distinct tubercles; lightly impressed medially; in dorsal view bearing two impressions on postero-lateral margins. Gaster with mostly simple setae, very few spatulate setae; terminal tergites have dense, lightly colored setae surrounded by dark setae; setae becoming less appressed towards terminal tergites and sternites; generally with strong confused reticulate sculpturing. First sternite and first tergite with confused-reticulate sculpturing; tergites I-IV have crenulate carinae bordering narrow shiny posterior margin.

MALE: Strongly appressed dark pilosity; mature males bicolored; head and mesosoma testaceous-orange and dark-ferruginous, in part due to darkened sculpturing; metasoma testaceous-orange (Fig. 3A); integument with weak to effaced rugulose sculpturing (Fig. 3A).

Head: Pilosity dark and appressed to weakly appressed and curved; head capsule generally with carinate-rugose sculpturing; but sparsely carinate and finely reticulate inferior

and lateral to frontal lobe; striate sculpture of head capsule in profile arranged nearly perpendicular to the longitudinal axis of the head (Fig. 3A; see also Fig. S6); head capsule in full-face view wider than long (Fig. 3B). Mandible with sparse, pale, and appressed setae; apical masticatory margin darker than rest of mandible; elongate-triangular and feebly sinuous; external margin feebly sinuate; prominent apical teeth; 4–6 mostly uniformly teeth. Clypeus absent to weakly sculptured; evenly rounded; narrow shiny anterior margin. Frons bulbous with weak to effaced carinate sculpturing across its entirety, forming two small mounds inferior to the frontal lobes. In lateral view, preocular carina occur near mandibular insertion, continue along inner margin of eye variably extending posterad. Frontal lobe with fine pilosity along margin but strongly curved setae on disc; strongly impressed medially; otherwise, smooth margin (Fig. 3B). Antennae covered with very fine lightly colored setae appressed (Fig. 3B); 13 segments; neck of scape and basal condyle visible (Fig. 3B); scape wide proximally, gently narrowing to apex. In full-face view lateral ocelli prominent and parallel to a shallow vertex impression (Fig. 3B). Supraocular projection absent or weak when, occurring directed posteriorly and near ocellus in full-face view.

Mesosoma: Setae strongly appressed throughout; sculpturing weak to effaced carinulate-rugulous, finely reticulate where carinulate-rugulous sculpturing absent. Pronotum with minute lateral spines projecting antero-laterally; median pronotal tubercle varying from clearly visible to greatly reduced, best seen laterally; forward-projecting median pronotal tubercle near mesoscutum and pronotal suture; inferior corner of pronotum, anterior to coxa I, carinae bear extremely reduced or absent inferior spine. Coxa mostly covered with light-colored setae. Coxa I with carinulate-rugulose sculpturing; coxa II with dark prominent setae posteriorly near trochanter; coxa I longer than coxa III, coxa II shortest. Mesoscutum, in lateral view, rounded and bulbous anteriorly, bulging over pronotal-mesoscutal suture. Mesoscutellar disc with two very small, posteriorly projecting spines. Propodeum with small posterior spines that are wider, or as wide at the base as long, projecting postero-laterally (Fig. 3A).

Wings: Overall pubescence fine. Forewing weakly bicolored; five cells; media-cubitus vein exceeds half-length of anal vein after the cubitus-anal vein proximally; length of radial sector-media greater than half the length of the radius radial sector. Hindwing with long fine setae on posterior margin, longer proximally than distally; uniform coloration, 6–8 hamuli.

Metasoma: Overall pilosity appressed; weakly sculptured; somewhat bicolored. Petiole with few curved and appressed setae dorsally; weakly costulate sculpturing; rounded; spiracle anterior to center; dorsally the lateral margins impressed, with anterior spine larger. Postpetiole with few curved and appressed setae dorsally; two ventral setae; in lateral view nearly rectangular; posterior margin shallowly impressed. Setae of first gastral tergite and sternite appressed; those on tergites 2–5, weakly appressed along posterior margins fine reticulate sculpturing. Pygostyle and genital opening densely covered with lightly colored setae.

Etymology

“Mikromelanos” is a singular, masculine adjective, compounded from the Greek μικρός (mikrós), meaning “small,” and μελανός (melanós), meaning “black” or “dark.” This etymology highlights the authors’ colloquial use of “little black” to describe the small darker queens of *M. mikromelanos*.

Comments

Although *M. mikromelanos* shares many similarities with *M. zeteki* (Figs. 2–5; [Weber, 1940](#); [Weber, 1958b](#); [Mayhé-Nunes & Brandão, 2007](#)), certain key characters allow us to easily distinguish the two species with a 20X loupe in the field. These key characters in *M. mikromelanos* are (i) the worker scapes extend past the occipital corners of the head capsule (extending only to the occipital corners in *M. zeteki*), (ii) gyne wing venation is ferruginous-brown in *M. mikromelanos* and testaceous-orange in *M. zeteki*, (iii) queens of *M. mikromelanos* are typically smaller and a dark reddish brown, where *M. zeteki* queens are larger and a bright reddish color, (iv) males are bi-colored, dark-ferruginous and testaceous-orange (uniform, testaceous-orange in *M. zeteki*), and (v) in general, all castes of *M. mikromelanos* are smaller than those of *M. zeteki*. Distinguishing between the gynes or queens of *M. mikromelanos* and *M. zeteki*, however, requires a microscope. Aside from size, it is most informative to look at sculpturing of the mesoscutum under a microscope: *M. mikromelanos* gynes have random reticulate sculpturing on the mesoscutum whereas *M. zeteki* have parallel sculpturing. In addition to color differences, males of the two species can be differentiated by the integumental sculpture near the eye. In the male of *M. mikromelanos* ocelli are small and in lateral view the striations follow the contours of the ventroposterior borders of the eye (Fig. 3A & S6). Whereas *M. zeteki* ocelli are large and striations fan outward from the ventroposterior corner of the head and are interrupted by the borders of the eye and the preocular carina, where they end (Fig. 5A & S10). A complete list of measurements is provided in the [Supplemental Information](#).

Biology

Mycetomoellerius mikromelanos is the most common ‘funnel *Mycetomoellerius*’ found on Pipeline Road, near Gamboa, Panama. Gynes establish nests from the start of the rainy season (May) into July. They nest in vertical clay embankments with entrances shaped like funnels (i.e., auricles) with flared margins ([Mueller & Wcislo, 1998](#); [Pérez-Ortega et al., 2010](#)). Colonies are often tucked under roots or overhangs and occur in high densities (as close as ~5cm apart) along creeks or are isolated in the forest at the base of trees. Colonies of *M. mikromelanos* have up to five vertically arranged chambers with single vertical tunnels between them. We removed the auricles from 16 nests and 15 were rebuilt to roughly the same size within seven days, suggesting the funnel structure appear to be biologically important (Figs. S7 & S8; also see [Mueller & Wcislo, 1998](#); [Schultz et al., 2002](#); [Pérez-Ortega et al., 2010](#); [Helms, Peeters & Fisher, 2014](#)). Several functional hypotheses have been proposed from physical barriers for army-ant raids to visual nest recognition cues. But nest entrances could also be involved in gas exchange currents that disperse colony odors or assist with colony respiration (see [Longino, 2005](#); [Helms, Peeters & Fisher, 2014](#)). Further research is necessary to clarify their biological function.



Figure 4 *Mycetomoellerius zeteki* worker (A–C) and gyne (D–F). (A) Worker profile. (B) Worker head full-face view; *FL* = Frontal Lobe spine; *CE* = Compound Eye; *Dsc* = Head capsule Disc; *Scp* = Scape. (C) Dorsal worker view. (D) gyne paratype full-face view; *AR* = Arcuate Ridge; *OS* = Occipital Spine; *Oc* = Ocelli. (E) Gyne lateral view, *Ha* = Hamuli. (F) Gyne dorsal view *Sclp* = sculpturing.

Full-size DOI: 10.7717/peerj.11622/fig-4

A variety of organisms exploit the resources of *M. mikromelanos* (e.g., fungal garden, shelter, brood). *Megalomyrmex adamsae* (Longino, 2010), a rare obligate social parasite (1–6% parasitism rate), forages on the host garden and brood and never leaves the nest of *M. mikromelanos* (Adams et al., 2012b). *Escovopsis Muchovej & Della Lucia, 1990*, an assumed micro-filamentous fungal parasite, is maintained at low levels due to specialized grooming behaviors used by workers of *M. mikromelanos* (Currie, Mueller & Malloch, 1999; Currie et al., 2003; Little et al., 2003; Little et al., 2006). Other fungi such as *Trichoderma* (Persoon, 1794) threaten the health of the garden and are managed by the ants (Currie et al., 2003; Little et al., 2006). There are also six Diapriinae (Hymenoptera: Diapriidae) morphospecies exploiting *M. mikromelanos*, but little natural history has been reported for these associations (but see Pérez-Ortega et al., 2010). Diapriinae parasitoid wasps infiltrate

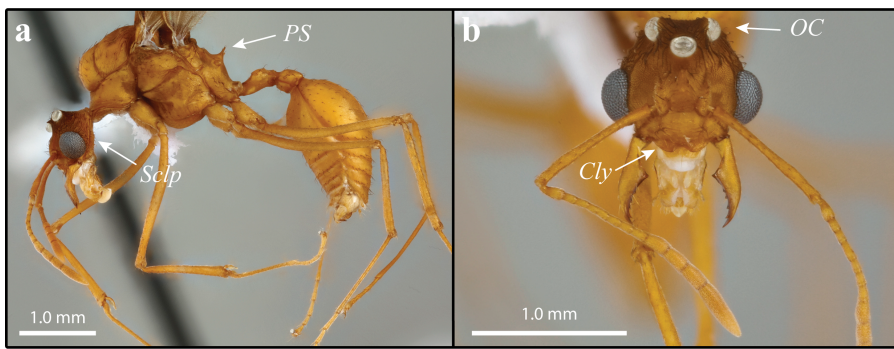


Figure 5 *Mycetomoellerius zeteki* male. (A) Profile, lateral view, *Sclp* = Sculpturing; *PS* = Propodeal Spine. (B) Head full-face view *Cly* = Clypeus impression corners; *OC* = Oceli.

[Full-size](#) DOI: [10.7717/peerj.11622/fig-5](https://doi.org/10.7717/peerj.11622/fig-5)

nests and parasitize host larvae, turning them black as the wasps develop internally. We found that mature wasp pupae can be prompted to eclose when disturbed or picked up and male *Acanthopria* sp. Ashmead 1895 tend to naturally emerge before *Acanthopria* females in captive colonies (ca. 10 days; deposited in the RMMA collection). We also found that *Mimopriella* sp. (Masner & García, 2002) can take up to six months to complete development in a laboratory-maintained colony. The mechanism behind this unusually slow growth is unknown. These symbionts highlight the known diversity of a species network that is reliant on *M. mikromelanos* for survival.

Mycetomoellerius zeteki (Weber, 1940)

Figs. 4 and 5 include *M. zeteki*.

Geographic range: Colombia, Costa Rica, Ecuador, Panama (Mayhé-Nunes & Brandão, 2007)

Label text: Separate labels for each specimen indicated by brackets (e.g., [Label 1] [Label 2]).

LECTOTYPE (here designated): Worker; [Barro Colorado. CANAL ZONE No. 856 NAWeber 1938] [*Trachymyrmex zeteki* Weber COTYPE] [USNMENT01129855].

Repository: Museum of Comparative Zoology, United States of America (MCZ).

PARALECTOTYPE (here designated, examined): Worker; [Barro Colo. I. Canal Zone No.756 NAWeber 1938] [M.C.Z. CoType 25619] [*T. zeteki* Weber Cotypes] [Harbor Islands Insect Database] [MCZ-ENT 00025619]. Repository: MCZ.

Additional material examined

Workers N = 24: MCZ: 1 specimen with the label data [Barro Colo. I. Canal Zone No756 NAWeber 1938 walking at 9 pm. Snyder-Molino 0-4.] [762 1 worker USNM]; 1 pin with 2 specimens [Barro Colo. I. Canal Zone No. 759 NAWeber 1938] [*T. balboai* Weber Cotypes]. NHMB: 1 specimen with the label data [Barro Colo. I C.Z. 3441 NAWeber] [*Trachymyrmex zeteki* Weber] [17.vi.56 3441] [ANTWEB CASENT

0912534]; NOTE: The NHMB pin bears a “type” label, but we assume it to be erroneous because the specimen was collected in 1956 and therefore cannot be part of Weber’s 1938 *M. zeteki* syntype series. USNM: 3 specimens sharing these label data [PANAMA: Pipeline Rd; 19 v 2010; Henrik H. De Fine Licht; nest series; river bank; underground; HDFL1952010-8] [see also cyro collections] [*Trachymyrmex* sp’s] [DO NOT REMOVE SI DB Reference Not a property tag T. Schultz, NMNH] USNMENT00752570 (1 pin with 2 specimens), USNMENT00752572. 16 specimens sharing these label data: [9.1624,-79.74802, PANAMA: Colón, Pipeline Rd, Bird Plot 4E19N, 70m, 29.vi.2010, Rachelle M.M. Adams, RMMA100629-15] [Formicidae Myrmicinae *Trachymyrmex zeteki*, [Weber, 1940](#), det. Cardenas, CR., 2018]. Repositories: USNM (4): USNMENT01129711, USNMENT01123714, USNMENT01123715, USNMENT01123716; MZSP (4): OSUC 640611, OSUC 640612, OSUC 640613, OSUC 640614; STRI (5): OSUC 640626, OSUC 640627, OSUC 640628, OSUC 640629, OSUC 640630; OSUC (3): OSUC 640601, OSUC 640602, OSUC 640603.

Gynes N = 9: Sharing these label data: [9.1624, -79.74802, PANAMA: Colón, Pipeline Rd, Bird Plot 4E19N, 70m, 29.vi.2010, Rachelle M.M. Adams, RMMA100629-15] [Formicidae Myrmicinae *Trachymyrmex zeteki*, [Weber, 1940](#), det. Cardenas, CR., 2018]. Repositories: USNM (4): USNMENT01123712, USNMENT01123717, USNMENT01123718, USNMENT01123719. MZSP (2): OSUC 640615, OSUC 640616; STRI (2): OSUC 640633, OSUC 640634; OSUC (1) OSUC 640604.

Males N = 11: USNM: 3 specimens sharing these label data [PANAMA: Pipeline Rd; 19 v 2010; Henrik H. De Fine Licht; nest series; riverbank; underground; HDFL1952010-8] [see also cyro collections] [*Trachymyrmex* sp’s] [DO NOT REMOVE SI DB Reference Not a property tag T. Schultz, NMNH] USNMENT00752568 and USNMENT00752570 (1 pin with 2 specimens). Sharing these label data: [9.1624, -79.74802, PANAMA: Colón, Pipeline Rd, Bird Plot 4E19N, 70m, 29.vi.2010, Rachelle M.M. Adams, RMMA100629-15] [Formicidae Myrmicinae *Trachymyrmex zeteki*, [Weber, 1940](#), det. Cardenas, CR., 2018]. Repositories: USNM (4): USNMENT01123713; USNMENT01123720; USNMENT01123721; USNMENT01123722; MZSP (1): OSUC 640617; STRI (2): OSUC 640633, OSUC 640634; OSUC (1): OSUC 640605.

Mycetomoellerius zeteki was originally described by [Weber \(1940\)](#) as *Trachymyrmex zeteki* from an accidental collection in dense shade on a slope near the lab on Barro Colorado Island, Panama Canal Zone ([Weber, 1940](#); [Mayhé-Nunes & Brandão, 2007](#)). In the same article Weber followed his description of *T. zeteki* with a description of *T. balboai* ([Weber, 1940](#)). These descriptions were based on a small series of workers from single collections. Weber noted similarities between the two species in his original descriptions. According to Weber, *T. zeteki* was distinctly smaller than *T. balboai*, paler in appearance, and the relative proportions of the thoracic spines differed. The character states that Weber used to differentiate the two species were later understood to represent variation within a single species and *T. balboai* was synonymized with *M. zeteki* ([Weber, 1958b](#)). In [Mayhé-Nunes & Brandão \(2007\)](#) revision of the *Trachymyrmex* “Jamaicensis group,” *M. zeteki* was placed in a subset of the “Iheringi group.” Distinct characteristics of the Jamaicensis group are the open antennal scrobes arising from the subparallel preocular and frontal carinae

(*Mayhé-Nunes & Brandão, 2007*), a character cited by *Solomon et al. (2019)* as applying to the entire genus *Mycetomoellerius*. Here we describe the gyne wing venation and males of *M. zeteki* and provide comparative morphology in the comments to delineate *M. zeteki* from *M. mikromelanos*. For complete descriptions of worker and gynes of *M. zeteki*, see *Weber (1940)*; *Weber (1958b)* and *Mayhé-Nunes & Brandão (2007)*.

Diagnosis: Measurements for all castes are found in **Table 2**, **Table S4**. Certain characters are useful for separating *M. zeteki* from *M. mikromelanos* sp. nov. However, due to the variability of the worker castes (e.g., mesosoma spines), intermediate character states occur in some individuals. The following characters are most useful.

Workers (1) cuticle ferrugineous (**Figs. 4A–4C**; dark-ferrugineous in *M. mikromelanos*); (2) integumental sculpture weakly irrorate (**Figs. 4A & 4B**; granulose irrorate sculpturing in *M. mikromelanos*); (3) frontal lobe with weakly crenulate margins and distinct antero-lateral spine (**Fig. 4B**; crenulations present and spines lacking in *M. mikromelanos*); (4) disc of head capsule between frontal carinae mostly lacking strongly hooked spatulate bi-colored setae (**Fig. 4B**; present in *M. mikromelanos*); (5) scape of antenna reaching occipital corners when lodged in antennal scrobe (**Fig. 4B**; surpassing occipital corners in *M. mikromelanos*); (6) convex margin of the compound eye extending past lateral border of head capsule by less than half of the eye area in full-face view (**Fig. 4B**; extending by more than half in *M. mikromelanos*).

Gyne (1) cuticle coloration ferrugineous (**Figs. 4D–4F**; dark-ferrugineous in *M. mikromelanos*); (2) supraocular tubercle separated from compound eye by a distance less than or equal to the eye length (**Fig. 4D**; more than or equal to eye length in *M. mikromelanos*); (3) small arcuate ridge superior to anterior ocellus with terminal ends directed antero-laterally (**Fig. 4D**; directed postero-laterally in *M. mikromelanos*); (4) lateral ocelli conspicuous in full-face view (**Fig. 4D**; partially obscured in *M. mikromelanos*); (5) mesosoma with sparse carinate sculpturing; mesoscutum with parallel-costulate sculpturing (**Fig. 4F**; random-reticulate in *M. mikromelanos*); (6) wing venation testaceous-orange brown (**Figs. 4E & 4F**; wings weakly ferrugineous-brown in *M. mikromelanos*); (7) hindwing with 5–8 hamuli (**Fig. 4E**; 7–9 in *M. mikromelanos*).

Male (1) coloration mostly uniform testaceous-orange (**Fig. 5A**; bicolored, head and mesosoma ferrugineous-brown with metasoma dark testaceous-orange in *M. mikromelanos*); (2) striations on head capsule fanning outward from ventroposterior corner of head, ending at the compound eye and preocular carina (**Fig. 5A & S10**; striations perpendicular to longitudinal axis in *M. mikromelanos*); sculpture prominent on posterior head capsule, minute to absent anteriorly (**Fig. 5A**; nearly complete sculpturing of head capsule in *M. mikromelanos*); (3) mandible larger compared to those of *M. mikromelanos*; (4) corners of clypeal emargination slightly angled (**Fig. 5B**; rounded in *M. mikromelanos*); (5) in full-face view; occipital corners of head capsule partially obscured by large ocelli (**Fig. 5B**; visible in *M. mikromelanos*); (6) propodeal spines longer than width of spine at base (**Fig. 5A**; wider at base than long in *M. mikromelanos*).

GYNE:

Wings: Overall pubescence fine. Tegula with dark appressed simple setae; testaceous-orange coloration; triangular; impressed face. Axillary sclerite with setae along ventral margins

and dark appressed setae on its face; flattened along distal margin. Forewing weakly tinted smokey grey, only slightly more so anteriorly than posteriorly; venation testaceous-orange/brown ([Fig. 4F](#)); five cells; length of radial sector-media vein less than half the length of radius-radial sector vein. Hindwing with long fine setae on posterior margin, longer proximally than distally; lightly tinted smokey grey, venation testaceous-orange/brown; 5-8 hamuli ([Figs. 4E & 4F](#)).

MALE: Dark and weakly appressed setae; mature males nearly uniform testaceous-orange color; darkened sculpturing on head capsule, otherwise integument generally weak to effaced carinulate-rugulose sculpturing ([Fig. 5A](#)).

Head: Poorly appressed curved dark setae; feebly darker than rest of body due to sculpturing; sculpturing carinulate-rugulose lateral and posterior to frontal lobes; sculpturing reduced posterior to median ocelli and in median portion of vertex; otherwise finely reticulate; striation on head capsule fanning outward from ventroposterior corner of head, ending at the compound eye and preocular carina ([Figs. 5A & 5B](#); see also [S10](#)); head capsule in full-face view wider than long ([Fig. 5B](#)). Mandible with fine and lightly colored setae; setae on external margin appressed; masticatory margin distinctly darker than rest of mandible; triangular and feebly sinuous; apical tooth prominent; with 5–7 dentate to denticulate teeth. Clypeal margin somewhat shiny; not evenly rounded; weak angle near clypeal emargination. Frons with carinulate-rugulose sculpturing forming two small mounds bearing curved setae inferior to frontal lobes; otherwise mostly smooth; somewhat bulbous. Preocular carina originating near mandibular insertion, continuing along inner margin of eye and extending variably posterad. Frontal lobe with fine pilosity along margin but dark simple setae on disc; lightly impressed medially; otherwise, smooth margin. Antenna with 13 segments; scape covered in fine and intermittent dark appressed setae; scape and basal condyle visible; scape wide proximally and gently tapering before widening sub-distally to apex ([Fig. 5B](#)). In full-face view ocelli large and distinct; central and lateral ocelli are prominent, large, and distinct; lateral ocelli parallel to the shallow vertex impression. Supraocular projection directed posteriorly, visible in full-face view.

Mesosoma: Somewhat appressed setae throughout; carinulate-rugulose sculpturing; weakly reticulate when carinulate-rugulose sculpturing absent. Pronotum with small lateral spine projecting anteriorly; minute to entirely absent spine occurs medially along anepisternum pronotal suture; inferior corner, near coxa I, with extremely reduced spine. Coxa covered mostly with lightly colored setae; weak carinulate sculpture. Coxa I with a few dark setae anteriorly. Coxa II with dark prominent setae mostly ventrally near trochanter. Length of coxa III equal to or longer than coxa I. Mesoscutum, in lateral view, rounded and bulbous anteriorly, bulging over pronotal-mesoscutal suture. Axilla hide part of scutoscutellar suture in lateral view. Mesoscutellar disc with two very small, posteriorly projecting spines ([Fig. 5A](#)). Propodeal spines as long or longer than width of base and projecting posteriorly ([Fig. 5A](#)).

Wings: Overall pubescence fine. Forewing weakly bicolored; possessing five cell; media-cubitus vein less than half length of anal vein after cubitus-anal proximally; length of radius-radial sector vein less than half the length of radial sector-media. Hindwing with

long fine setae on posterior margin, more so proximally than distally; uniform in coloration; 4–7 hamuli.

Metasoma: Mostly weakly appressed simple and subtly curved setae; uniform coloration; poorly sculptured. Petiole with curved setae dorsally; costulate sculpturing if present; node rounded; in profile spiracle present medially at anterior margin; in dorsal view antero-lateral tumuli flanking a flattened medial projection. Postpetiole sculpturing finely reticulate if present; posterior ventral side with spine present varying in length from absent to almost as long as postpetiole; in lateral view nearly square; shallow posterior impression. Gaster setae sparse and appressed; sculpturing finely reticulate; sternites and tergite setae sparse and appressed; sternite and tergite 2–5 with dark setae along posterior margins. Pygostyle and genital opening covered with lightly colored setae.

Comments

A specimen of *M. zeteki* deposited at the Natural History Museum, Basel Switzerland bears a “cotype” (i.e., syntype) label in error. The data label reads as follows ‘[Barro Colo. I C.Z. 3441 NAWeber] [17.vi.56 3441] [*Trachymyrmex zeteki* Weber] [ANTWEBCASENT0912534] [type].’ It is not possible that this specimen, collected in 1956, 18 years after the *M. zeteki* type series was collected, is a type specimen of that species. While this specimen could be part of the material examined in [Weber, 1958b](#) *balboai-zeteki* synonymy, no repositories were mentioned. This specimen was not treated as a syntype for this study. For a complete description of the workers and gyne of *M. zeteki*, see [Mayhé-Nunes & Brandão \(2007\)](#). Certain key characters allow us to easily distinguish *M. zeteki* from *M. mikromelanos* with a 20X loupe in the field. For *M. zeteki* these characters are (i) in workers of *M. zeteki*, the scapes reach the occipital corners of the head capsule but do not extend past them, whereas in *M. mikromelanos*, they extend past the head capsule when lodged in the antennal scrobe, (ii) the queens of *M. zeteki* are comparatively larger than those of *M. mikromelanos* and are typically bright reddish in color whereas *M. mikromelanos* are generally a darker reddish brown, (iii) gyne wing venation is testaceous-orange in *M. zeteki* and ferrugineous-brown in *M. mikromelanos*, (iv) males are uniform in color and testaceous-orange (bicolored dark-ferrugineous and testaceous-orange in *M. mikromelanos*), and (v) in general all castes of *M. zeteki* are larger than *M. mikromelanos*. It is necessary to note that workers from incipient colonies of *M. zeteki* tend to resemble workers of *M. mikromelanos* and require careful attention to the additional variable characters. A complete list of measurements can be found in the [Supplemental Information](#).

Biology

Most reports of *M. zeteki* are most likely accounts of *M. mikromelanos* ([Appendix Table S1](#)). *Mycetomoellerius zeteki* is rare relative to *M. mikromelanos* in the Canal Zone near Gamboa, Panama. For example, we only located two colonies of *M. zeteki* near the type locality on Barro Colorado Island, and one colony at El Llano ca. 40 km east of the canal. On the mainland we have found mixed sites of both species and a single creek with only *M. zeteki* present (Rio Mendoza, ca. 1 km North of Rio La Seda), but when the two species occur together, *M. zeteki* always occurs at comparably lower densities. While some *M. zeteki*

samples are indicated to be collected from Nicaragua we examined seven specimens from JTL and three specimens were morphologically distinct from the Panamanian *M. zeteki* and *M. mikromelanos*. *Mycetomoellerius zeteki* and *M. mikromelanos* are similar morphologically and biologically and this has led to confusion between these sister species. In both species, gynes establish their nests from the start of the rainy season (around May) into July. Nests can be found on the same clay embankments with indistinguishable auricles with up to five chambers. In the five mature *M. zeteki* nests we excavated, each had two tunnels connecting each chamber. In contrast *M. mikromelanos* has only one tunnel connecting them and there are likely other architectural differences, such as volume and internal auricle shape, but more colonies of *M. zeteki* need to be examined.

Mycetomoellerius zeteki and *M. mikromelanos* also have a similar range of symbionts. *Megalomyrmex adamsae* associates with *M. zeteki*, foraging on host garden and brood, and never leaves the host nest (Adams et al., 2012b). An *Escovopsis* fungal parasite attacks the fungal garden. Garden maintenance behavior also appears similar as *M. zeteki* forms infrabuccal pellet piles like *M. mikromelanos* (Little et al., 2003). We have documented the first Diapriidae wasp parasitizing the brood of *M. zeteki*. In a laboratory colony (CRC170519-01), we observed a male wasp of *Mimopriella* sp. (deposited in the RMMA collection) emerge on May 19th, 2017, and a female 10 days later. The live colony had characteristically black larvae when collected. While some natural history has been documented, there is still much more to be discovered about the symbionts, nest architecture, and general biology of *M. zeteki*.

DISCUSSION

Based on multiple lines of evidence, we have shown that the new species *M. mikromelanos* is a well-studied cryptic species that has been confused with *M. zeteki* for decades. We accomplished this by examining morphology and morphometrics of all castes, analyzing the behavior of workers, comparing worker volatile compounds, and comparing DNA sequence data. Interestingly, we also determined that the published genome (Nygaard et al., 2016) belongs to the newly described species *M. mikromelanos*. Our results underscore the importance of species discovery by emphasizing the value of an integrative taxonomic approach, the effect of species delineation on biodiversity, and the necessity of properly vouchered specimens.

While historical taxonomic work generally relied on morphological characters alone to delineate and typify species, modern taxonomy more often utilizes other biological evidence (Dayrat, 2005; Schlick-Steiner et al., 2010). An integrative approach is frequently used to overcome the challenges of cryptic species, especially those lacking clear morphological characters adequate for recognizing species boundaries. Complementary lines of evidence in addition to morphology (e.g., behavioral, molecular, chemical, ecological, etc.) increase our confidence in species descriptions and reveal the intricacies of those species' biology (Dayrat, 2005). Employing this approach, we analyzed biologically relevant evidence along with key morphological characters—summarized in the diagnoses of *M. mikromelanos* and *M. zeteki*—that proved useful for distinguishing the two species. These are best observed

using a standard dissection microscope but can also be detected with a 20X loupe. Another line of evidence is provided by our behavioral analysis. It was initially assumed that tempo would reflect behavioral differences observed in the field, where *M. zeteki* appeared ‘aggressive’ and *M. mikromelanos* ‘passive’. However, we found that these two sibling species show differences in tempo, the rate of movement, rather than in aggressive or passive behaviors. Lastly, our chemical analysis also shows species-specific differences in the abundance of volatile compounds for most analyzed workers of both species. The combined evidence supports the existence of two distinct and closely related sympatric species in the Panama Canal Zone, *M. mikromelanos* and *M. zeteki*. The recognition of two species adds to our understanding of the multiple symbiotic relationships involving each species. It should be noted that, although it appears fairly certain that *M. mikromelanos* represents a single, well-supported species (Fig. 1E), the possibility remains that *M. zeteki* as currently defined may actually consist of two or more cryptic species. In Fig. 1E, all the samples of *M. mikromelanos* form a very well-supported clade whereas the monophyly of the two *M. zeteki* samples is poorly supported. This is also reflected in a larger phylogeny where the same two *M. zeteki* samples are monophyletic but have similarly poor support and long branch lengths (see Fig. 2 of Solomon *et al.*, 2019).

Species delimitation is essential not only for descriptive biology, but also for understanding the levels of biodiversity. In this context, species represent units of study that help us comprehend ecological and evolutionary principals. These include, but are not limited to, genetic diversity, adaptation, and broad-scale community interactions. Fungus-growing ants are an intriguing group for the study of biodiversity given their coevolutionary history with their fungal cultivars (Mehdiabadi *et al.*, 2012), their many other symbiotic relationships (Mueller, Rehner & Schultz, 1998; Currie, Mueller & Malloch, 1999; De Fine Licht & Boomsma, 2014), and the role fungus-growing ants play as ecosystem engineers (Jones, Lawton & Shachak, 1994; Folgarait, 1998; Meyer *et al.*, 2011; Meyer *et al.*, 2013). However, the distributions and ecological roles of most non-leaf-cutting attines in neotropical environments is still poorly studied (but see Leal & Oliveira, 2000; Vasconcelos, Araújo & Mayhé-Nunes, 2008; Tschinkel & Seal, 2016). For example, during the summer of 2018 we searched BCI, Fort Sherman, and El Llano (ca. 15, 35, and 80 km from Pipeline Road, respectively) for both *M. mikromelanos* and *M. zeteki*. Yet after searching kilometers of trails and creeks on BCI we were unable to locate any *M. mikromelanos* colonies, and only located two *M. zeteki* colonies on BCI and one at El Llano. No *M. mikromelanos* were found outside of the regularly sampled Gamboa Forest and Pipeline Road areas with the exception of a sample collected by Dr. Jack Longino in the Darien Provence of Panama in 2015. Regardless of our uncertainty of *M. mikromelanos*’ distribution outside of the Canal Zone, we do have some familiarity with *M. mikromelanos*’ and *M. zeteki*’s symbiotic associations. For example, they maintain similar relationships with social parasites, garden pathogens, and parasitoids (see “Biology” in species descriptions). Describing *M. mikromelanos* has enhanced our understanding of the symbiotic relationships of both species and raises more questions about them and their associates. Further research clarifying the natural history of these species and their symbionts will help us discern their ecological roles and contribute to our understanding of biodiversity in the Panama Canal Zone.

Genetic patterns and genetic diversity are another important aspect of biodiversity. Together they can inform understanding of the dispersal capabilities of species ([Sanetra & Crozier, 2003](#); [Sanllorente, Ruano & Tinaut, 2015](#); [Boulay et al., 2017](#); [Helms IV, 2018](#)) biogeographic histories ([Branstetter et al., 2017](#); [Mueller et al., 2017](#); [Mueller et al., 2018](#)), demographic history ([Castilla et al., 2016](#)), and evolutionary patterns ([Baer & Boomsma, 2004](#); [Schultz & Brady, 2008](#); [Nygaard et al., 2016](#); [Mueller et al., 2018](#)). Modern molecular genetic tools enable researchers to study populations and their patterns at broad biogeographic ranges. According to several studies, higher attine ants are believed to grow two clades of fungi ([Solomon et al., 2019](#); [Schultz et al., 2015](#); [Ješovník & Schultz, 2017](#); [Shik et al., 2021](#); [Mueller et al., 2018](#)). Still, there is not a one-to-one association or complete phylogenetic congruence between higher attine ants and their cultivars ([Schultz et al., 2015](#); [Mueller et al., 2018](#)). Including a broader sampling of species revealed that a lower attine species (e.g., *Apterostigma megacephala* ([Lattke, 1999](#))) also cultivates a *L. gongylophorus* higher attine garden ([Schultz et al., 2015](#)). Furthermore, multiple cultivar strains or haplotypes can be cultivated by the same or different ant species from the same location ([Green, Mueller & Adams, 2002](#); [Shik et al., 2021](#)). As in most scientific endeavors, new knowledge of ant-fungus associations requires constant updating of older models ([Chapela et al., 1994](#); [Mueller & Wcislo, 1998](#); [Schultz & Brady, 2008](#); [Mehdiabadi & Schultz, 2010](#)). This process generates a deeper and more complicated picture of the biogeographic patterns observed in populations of the higher attines. Well-designed population-level analyses of the 61 non-leaf-cutting higher attine ant species (e.g., *Mycetomoellerius*, *Paratrachymyrmex*, *Trachymyrmex*, *Xerolitor*, and *Sericomyrmex*) would further refine our understanding of coevolution in the fungus-growing ants. *Mycetomoellerius mikromelanos* is well suited for such population-genetic analyses for a few reasons: it is abundant in the Canal Zone and easily located given its characteristic auricle nest entrance, it is sympatric with its sister species *M. zeteki*, and it has a published genome ([Nygaard et al., 2016](#)). Originally named *Trachymyrmex zeteki* on GenBank (([Nygaard et al., 2016](#)); GenBank accession: [GCA_001594055.1](#)), we confirm in this study based on published nuclear gene sequences (see phylogenetic analysis) and morphological evidence of vouchers (see taxonomy; [Figs. S11 & S12](#)) that it is the genome of *M. mikromelanos*.

The published genome of *M. mikromelanos* highlights the importance of species identification and voucher specimen deposition. Physical vouchers provide reproducibility and confidence in published findings. Curating physical collections, naming species, and creating molecular databases still depend on non-molecular taxonomic work ([Dayrat, 2005](#); [Turney et al., 2015](#)). We found that the incidence of reported vouchering for *M. zeteki* or *M. cf. zeteki*, based on our literature review, is higher than what is typically found in the field of entomology (44% versus 35%; [Turney et al., 2015](#)). This could be due to the exponential increase in research focusing on attines and collaborations with skilled taxonomists over the past thirty to forty years. We argue that more effort in voucher deposition is needed and that this is especially true when genomic information is published. Genomic resources are frequently used to compare and characterize gene functions (e.g., [Lee et al., 2017](#); [Nolasco et al., 2018](#); [Wang et al., 2019](#)). Incomplete taxonomic information can lead to a series of misguided future studies.

CONCLUSIONS

Given the abundance of *M. mikromelanos* in the Panama Canal Zone, we expect that the majority of researchers who believe they have studied *M. zeteki* have studied *M. mikromelanos* instead ([Appendix Table S1](#)). We encourage these researchers to mount specimens, confirm the species identification, and deposit the vouchers in a well-curated and accessible natural history museum collection. Our hope is that our results will encourage voucher deposition, even for common species such as *M. mikromelanos*. While physical voucher specimens are not typically required by journal policy or by reviewers ([Turney et al., 2015](#)), our findings draw attention to why this is important. We recommend that investigators include voucher specimen preparation and deposition as part of their normal research practice and instill this principle in mentees and colleagues.

ACKNOWLEDGEMENTS

We thank the staff and researchers at the Smithsonian Tropical Research Institute (STRI) for logistical support and the Autoridad Nacional del Ambiente y el Mar for permission to sample and export ants. Some live colonies were provided by our colleague Morten Schiøtt, along with Matt F. Fisher and Konstantinos Giampoudakis in conjunction with the graduate course Tropical Behavioral Ecology and Evolution (TBEE) at STRI, hosted by the Centre for Social Evolution, University of Copenhagen and STRI in 2011 and by The Ohio State University and STRI in 2017 and 2019. Specimens were generously loaned from the Museum of Comparative Zoology, Harvard, Cambridge, Massachusetts, the National Museum of Natural History, Washington, D.C., The Natural History Museum Basel, Basel, Switzerland, and Jack Longino. We thank Panagiotis Sapountzis for assistance with the etymology, Luciana Musetti and Sarah Hemly from the Triplehorn Insect Collection, and David Culver, Joan M. Herbers, and Steven Passoa for microscopy support. We thank Alexander Wild for assistance with establishing an Adams *Mega*. Lab automontage system. We are grateful to Christopher Wilson, Marymegan Daly, and the Adams *Mega* Ant Lab peers for improving this work with extensive editing, conversation, and encouragement. We thank the reviewers Pepijn Kooij, Rodrigo Feitosa, and Monica Ulyssea and the editor Joeseph Gillespie for helpful comments on the final draft of the manuscript. Lastly, we dedicate this work to the late Christopher Wilson, who will be missed.

ADDITIONAL INFORMATION AND DECLARATIONS

Funding

Ted Schultz was supported by the National Science Foundation grants DEB 1927224 and 1654829. The funders had no role in study design, data collection and analysis, decision to publish, or preparation of the manuscript.

Grant Disclosures

The following grant information was disclosed by the authors:

National Science Foundation: DEB 1927224, 1654829.

Competing Interests

The authors declare there are no competing interests.

Author Contributions

- Cody Raul Cardenas conceived and designed the experiments, performed the experiments, analyzed the data, prepared figures and/or tables, authored or reviewed drafts of the paper, generated R code for morphometric and behavioral analysis, and approved the final draft.
- Amy Rongyan Luo conceived and designed the experiments, performed the experiments, analyzed the data, prepared figures and/or tables, authored or reviewed drafts of the paper, generated R code behavioral analysis, and approved the final draft.
- Tappey H. Jones performed the experiments, analyzed the data, authored or reviewed drafts of the paper, and approved the final draft.
- Ted R. Schultz analyzed the data, authored or reviewed drafts of the paper, and approved the final draft.
- Rachelle M.M. Adams conceived and designed the experiments, performed the experiments, analyzed the data, prepared figures and/or tables, authored or reviewed drafts of the paper, and approved the final draft.

Ethics

The following information was supplied relating to ethical approvals (i.e., approving body and any reference numbers):

The Smithsonian Tropical Research Institute approved the project named "Behavioral Ecology and Systematics of the Fungus-growing Ants and Their Symbionts (#4056)" to be conducted in Panama in its nature preserves.

Field Study Permissions

The following information was supplied relating to field study approvals (i.e., approving body and any reference numbers):

Colony collection and field work were approved by the Smithsonian Tropical Research Institute and the Autoridad Nacional del Ambiente y el Mar (Permiso de Colecta Científica 2017: SPO-17-173 and 2018: SE/AB-1-18).

The United States Department of Agriculture approved the import of specimens and live colonies maintained at an approved facility (permit: APHIS P526P-16-02785; facility #4036).

Data Availability

The following information was supplied regarding data availability:

Raw data and associated R code for morphometrics, behavior, phylogenetic, and chemical analyses are available in the [Supplemental Files](#) and at GitHub: https://github.com/crcardenas/Mycetomoellerius_spn.

All specimens examined and the associated repositories are in the [Supplemental File](#).

New Species Registration

The following information was supplied regarding the registration of a newly described species:

Publication LSID: urn:lsid:zoobank.org:pub:737E04E5-5A8F-48F6-BE32-ADC1028927B6

Mycetomoellerius mikromelanos sp. n. LSID urn:lsid:zoobank.org:act:B6BABA13-708F-44D8-AD2C-F4D5B8FB03E8.

Supplemental Information

Supplemental information for this article can be found online at <http://dx.doi.org/10.7717/peerj.11622#supplemental-information>.

REFERENCES

- Adams RMM, Jones TH, Jeter AW. 2010.** Male specific tyramides from three additional myrmicine genera. *Biochemical Systematics and Ecology* **38**:454–456 DOI [10.1016/j.bse.2010.03.008](https://doi.org/10.1016/j.bse.2010.03.008).
- Adams RMM, Jones TH, Jeter AW, De Fine Licht HH, Schultz TR, Nash DR. 2012a.** A comparative study of exocrine gland chemistry in *Trachymyrmex* and *Sericomyrmex* fungus-growing ants. *Biochemical Systematics and Ecology* **40**:91–97 DOI [10.1016/j.bse.2011.10.011](https://doi.org/10.1016/j.bse.2011.10.011).
- Adams RMM, Liberti J, Illum AA, Jones TH, Nash DR, Boomsma JJ. 2013.** Chemically armed mercenary ants protect fungus-farming societies. *Proceedings of the National Academy of Sciences of the United States of America* **110**:15752–15757 DOI [10.1073/pnas.1311654110](https://doi.org/10.1073/pnas.1311654110).
- Adams RMM, Shah K, Antonov LD, Mueller UG. 2012b.** Fitness consequences of nest infiltration by the mutualist-exploiter *Megalomyrmex adamsae*. *Ecological Entomology* **37**:453–462 DOI [10.1111/j.1365-2311.2012.01384.x](https://doi.org/10.1111/j.1365-2311.2012.01384.x).
- Altschul SF, Gish W, Miller W, Myers EW, Lipman DJ. 1990.** Basic local alignment search tool. *Journal of Molecular Biology* **215**:403–410 DOI [10.1016/S0022-2836\(05\)80360-2](https://doi.org/10.1016/S0022-2836(05)80360-2).
- Baer B, Boomsma JJ. 2004.** Male reproductive investment and queen mating-frequency in fungus-growing ants. *Behavioral Ecology* **15**:426–432 DOI [10.1093/beheco/arh025](https://doi.org/10.1093/beheco/arh025).
- Bates D, Mächler M, Bolker B, Walker S. 2015.** Fitting linear mixed-effects models using lme4. *Journal of Statistical Software* **67**:1–48 DOI [10.18637/jss.v067.i01](https://doi.org/10.18637/jss.v067.i01).
- Besheres SN, Traniello JFA. 1996.** Polyethism and the adaptiveness of worker size variation in the attine ant *Trachymyrmex septentrionalis*. *Journal of Insect Behavior* DOI [10.1007/BF02213724](https://doi.org/10.1007/BF02213724).
- Boomsma JJ. 2007.** Kin selection versus sexual selection: why the ends do not meet. *Current Biology* **17**:673–683 DOI [10.1016/j.cub.2007.06.033](https://doi.org/10.1016/j.cub.2007.06.033).
- Boudinot BE, Sunnicht TP, Adams RMM. 2013.** Central American ants of the genus *Megalomyrmex* Forel (Hymenoptera: Formicidae): six new species and keys to workers and males. *Zootaxa* **3732**:1–82 DOI [10.11164/zootaxa.3732.1.1](https://doi.org/10.11164/zootaxa.3732.1.1).

- Boulay R, Aron S, Cerdá X, Doums C, Graham P, Hefetz A, Monnin T.** 2017. Social life in arid environments: the case study of *Cataglyphis* ants. *Annual Review of Entomology* **62**:305–321 DOI [10.1146/annurev-ento-031616-034941](https://doi.org/10.1146/annurev-ento-031616-034941).
- Brandão CRF, Mayhé-Nunes AJ.** 2007. A phylogenetic hypothesis for the *Trachymyrmex* species groups, and the transition from fungus-growing to leaf-cutting in the Attini. *Memoirs of the American Entomological Institut* **80**:73–87 DOI [10.1533/9781845696382.2.267](https://doi.org/10.1533/9781845696382.2.267).
- Branstetter MG, Ješovník A, Sosa-calvo J, Lloyd MW, Faircloth BC, Brady SGS, Schultz TR.** 2017. Dry habitats were crucibles of domestication in the evolution of agriculture in ants. *Proceedings of the Royal Society B: Biological Sciences* **284**:1–10 DOI [10.1098/rspb.2017.0095](https://doi.org/10.1098/rspb.2017.0095).
- Cafaro MJ, Currie CR.** 2005. Phylogenetic analysis of mutualistic filamentous bacteria associated with fungus-growing ants. *Canadian Journal of Microbiology* **51**:441–446 DOI [10.1139/w05-023](https://doi.org/10.1139/w05-023).
- Cardenas CR, De Milto AD, Schultz TR, Adams RMM.** 2016. A revisionary study of *Trachymyrmex zeteki* (Formicidae: Attini) and description of a new species, *Trachymyrmex fovater* sp. n. In: *The Ohio State University 2016 Fall Undergraduate Poster Forum, 10th*. Columbus: Knowledge Bank.
- Castilla AR, Pope N, Jaffé R, Jha S.** 2016. Elevation, not deforestation, promotes genetic differentiation in a pioneer tropical tree. *PLOS ONE* **11**:1–22 DOI [10.1371/journal.pone.0156694](https://doi.org/10.1371/journal.pone.0156694).
- Chapela I, Rhener S, Schultz TR, Mueller UG.** 1994. Evolutionary history of the symbiosis between fungus-growing ants and their fungi. *Science* **266**:1691–1694.
- Chapman BB, Thain H, Coughlin J, Hughes WOH.** 2011. Behavioural syndromes at multiple scales in *Myrmica* ants. *Animal Behaviour* **82**:391–397 DOI [10.1016/j.anbehav.2011.05.019](https://doi.org/10.1016/j.anbehav.2011.05.019).
- Cristiano MP, Cardoso DC, Sandoval-Gómez VE, Simões Gomes FC.** 2020. *Amoimyrmex* Cristiano, Cardoso, & Sandoval, gen. nov. (Hymenoptera: Formicidae): a new genus of leaf-cutting ants revealed by multilocus molecular phylogenetic and morphological analyses. *Austral Entomology* **59**:643–676 DOI [10.1111/aen.12493](https://doi.org/10.1111/aen.12493).
- Currie CR, Mueller UG, Malloch D.** 1999. The agricultural pathology of ant fungus gardens. *Proceedings of the National Academy of Sciences of the United States of America* **96**:7998–8002.
- Currie CR, Wong B, Stuart AE, Schultz TR, Rehner SA, Mueller UG, Sung GH, Spatafora JW, Straus NA.** 2003. Ancient tripartite coevolution in the attine ant-microbe symbiosis. *Science* **299**:386–388 DOI [10.1126/science.1078155](https://doi.org/10.1126/science.1078155).
- Dayrat B.** 2005. Towards integrative taxonomy. *Biological Journal of the Linnean Society* **85**:407–415 DOI [10.1111/j.1095-8312.2005.00503.x](https://doi.org/10.1111/j.1095-8312.2005.00503.x).
- De Fine Licht HH, Boomsma JJ.** 2010. Forage collection, substrate preparation, and diet composition in fungus-growing ants. *Ecological Entomology* **35**:259–269 DOI [10.1111/j.1365-2311.2010.01193](https://doi.org/10.1111/j.1365-2311.2010.01193).

- De Fine Licht HH, Boomsma JJ.** 2014. Variable interaction specificity and symbiont performance in Panamanian *Trachymyrmex* and *Sericomyrmex* fungus-growing ants. *BMC Evolutionary Biology* **14**:1–10 DOI [10.1186/s12862-014-0244-6](https://doi.org/10.1186/s12862-014-0244-6).
- Fabricus JC.** 1804. *Systema Piezatorum secundum ordines, genera, species, adjectis synonymis, locis, observationibus, descriptionibus*. Brunswick: C. Reichard.
- Folgarait PJ.** 1998. Ant biodiversity and its relationship to ecosystem functioning: a review. *Biodiversity and Conservation* **7**:1221–1244 DOI [10.1023/A:1008891901953](https://doi.org/10.1023/A:1008891901953).
- Forel A-H.** 1983. Note sur les Attini. *Annales de la Société Entomologique Belge* **37**:586–607.
- Glon MG, Thoma RF, Daly M, Freudenstein JV.** 2019. *Lacunicambarus chimera*: a new species of burrowing crayfish (Decapoda: Cambaridae) from Illinois, Indiana, Kentucky, and Tennessee. *Zootaxa* **4544**(4):451–478.
- Green AM, Mueller UG, Adams RMM.** 2002. Extensive exchange of fungal cultivars between sympatric species of fungus-growing ants. *Molecular Ecology* **11**:191–195 DOI [10.1046/j.1365-294X.2002.01433.x](https://doi.org/10.1046/j.1365-294X.2002.01433.x).
- Hamilton N, Jones TH, Shik JZ, Wall B, Schultz TR, Blair HA, Adams RMM.** 2018. Context is everything: mapping *Cyphomyrmex*-derived compounds to the fungus-growing ant phylogeny. *Chemeocology* **28**:137–144 DOI [10.1007/s00049-018-0265-5](https://doi.org/10.1007/s00049-018-0265-5).
- Harris RA.** 1979. A glossary of surface sculpturing. *Occasional Papers in Entomology* **28**:1–34 DOI [10.5281/zenodo.26215](https://doi.org/10.5281/zenodo.26215).
- Helms IV JA.** 2018. The flight ecology of ants (Hymenoptera: Formicidae). *Myrmecological News* **26**:19–30.
- Helms JA, Peeters C, Fisher BL.** 2014. Funnels, gas exchange and cliff jumping: natural history of the cliff dwelling ant *Malagidris sofina*. *Insectes Sociaux* **61**:357–365 DOI [10.1007/s00040-014-0360-8](https://doi.org/10.1007/s00040-014-0360-8).
- Hoang DT, Chernomor O, Von Haeseler A, Minh BQ, Vinh LS.** 2018. UFBoot2: improving the ultrafast bootstrap approximation. *Molecular Biology and Evolution* **35**:518–522 DOI [10.5281/zenodo.854445](https://doi.org/10.5281/zenodo.854445).
- International Commission on Zoological Nomenclature.** 1999. *International code of zoological nomenclature*. London: The International Trust for Zoological Nomenclature.
- Ješovník A, Schultz TR.** 2017. Revision of the fungus-farming ant genus *Sericomyrmex* Mayr (Hymenoptera, Formicidae, Myrmicinae). *ZooKeys* **670**:1–109 DOI [10.3897/zookeys.670.11839](https://doi.org/10.3897/zookeys.670.11839).
- Ješovník A, Sosa-calvo J, Lopes CT, Vasconcelos HL, Schultz TR.** 2013. Nest architecture, fungus gardens, queen, males and larvae of the fungus-growing ant *Mycetagoicus inflatus* Brandão & Mayhé-Nunes. *Insectes Sociaux* **60**:531–542 DOI [10.1007/s00040-013-0320-8](https://doi.org/10.1007/s00040-013-0320-8).
- Jones CG, Lawton JH, Shachak M.** 1994. Organisms as ecosystem engineers. *Oikos* **69**:373–386 DOI [10.2307/3545850](https://doi.org/10.2307/3545850).
- Kalyaanamoorthy S, Minh BQ, Wong TKF, Von Haeseler A, Jermiin LS.** 2017. ModelFinder: fast model selection for accurate phylogenetic estimates. *Nature Methods* **14**:587–589 DOI [10.1038/nmeth.4285](https://doi.org/10.1038/nmeth.4285).

- Lattke JE.** 1999. A new species of fungus-growing ant and its implications for attine phylogeny (Hymenoptera: Formicidae). *Systematic Entomology* **24**:1–6.
- Leal IR, Oliveira PS.** 2000. Foraging ecology of attine ants in a Neotropical savanna: seasonal use of fungal substrate in the cerrado vegetation of Brazil. *Insectes Sociaux* **47**:376–382 DOI [10.1007/PL00001734](https://doi.org/10.1007/PL00001734).
- Lee J, Suryaningtyas IT, Yoon T, Min J, Park H, Kim H.** 2017. Transcriptomic analysis of the hepatopancreas induced by eyestalk ablation in shrimp, *Litopenaeus vannamei*. *Comparative Biochemistry and Physiology - Part D* **24**:99–110 DOI [10.1016/j.cbd.2017.08.004](https://doi.org/10.1016/j.cbd.2017.08.004).
- Leite LAR.** 2012. Mitochondrial pseudogenes in insect DNA barcoding: differing points of view on the same issue. *Biota Neotropica* **12**:301–308.
- Little AEF, Murakami T, Mueller UG, Currie CR.** 2003. The infrabuccal pellet piles of fungus-growing ants. *Die Naturwissenschaften* **90**:558–562 DOI [10.1007/s00114-003-0480](https://doi.org/10.1007/s00114-003-0480).
- Little AEF, Murakami T, Mueller UG, Currie CR.** 2006. Defending against parasites: fungus-growing ants combine specialized behaviours and microbial symbionts to protect their fungus gardens. *Biology Letters* **2**:12–16 DOI [10.1098/rsbl.2005.0371](https://doi.org/10.1098/rsbl.2005.0371).
- Lizidatti CS.** 2006. Biologia, arquitetura de ninhos e coleta de substratos no Cerrado por formigas cultradoras de fungo, *Trachymyrmex holmgreni* Wheeler 1925 (Hymenoptera, Formicidae, Attini). Masters Dissertation, Universidade Estadual Paulista, São Paulo, Brazil.
- Longino JT.** 2005. Complex nesting behavior by two Neotropical species of the ant genus *Stenamma* (Hymenoptera: Formicidae). *Biotropica* **37**:670–675.
- Longino JT.** 2010. A taxonomic review of the ant genus *Megalomyrmex* Forel (Hymenoptera: Formicidae) in Central America. *Zootaxa* **2720**:35–58 DOI [10.11646/zootaxa.2720.1.3](https://doi.org/10.11646/zootaxa.2720.1.3).
- Masner L, García JR.** 2002. The genera of Diapriinae (Hymenoptera: Diapriidae) in the New World. *Bulletin of the American Museum of Natural History* **268**:1–138 DOI [10.1206/0003-0090\(2002\)268<0001:TGODHD>2.0.CO;2](https://doi.org/10.1206/0003-0090(2002)268<0001:TGODHD>2.0.CO;2).
- Mayhé-Nunes AJ, Brandão CRF.** 2002. Revisionary studies on the Attine ant genus *Trachymyrmex* Forel, Part 1: definition of the genus and the *Opulentus* group (Hymenoptera: Formicidae). *Sociobiology* **40**:667–698 DOI [10.1111/j.1744-7429.2005.00085.x](https://doi.org/10.1111/j.1744-7429.2005.00085.x).
- Mayhé-Nunes AJ, Brandão CRF.** 2005. Revisionary studies on the Attine ant genus *Trachymyrmex* Forel. Part 2: the *Iheringi* group (Hymenoptera: Formicidae). *Sociobiology* **45**:271–305.
- Mayhé-Nunes AJ, Brandão CRF.** 2007. Revisionary studies on the attine ant genus *Trachymyrmex* Forel. Part 3: the *Jamaicensis* group (Hymenoptera: Formicidae). *Zootaxa* **1444**:1–21.
- Mayr G.** 1865. Formicidae. In: *Novara Expedition 1865*. Reise der Österreichischen Fregatte Novara um die Erde in den Jahren 1857, 1858, 1859. Zoologischer Theil. Bd. II. Abt. 1. Wein: K. Gerol's Son, 83.

- McCune B, Grace JB.** 2002. *Analysis of ecological communities*. Gleneden Beach, Oregon: MjM Software Desig.
- Mehdiabadi NJ, Mueller UG, Brady SG, Himler AG, Schultz TR.** 2012. Symbiont fidelity and the origin of species in fungus-growing ants. *Nature Communications* **3**:1–7 DOI [10.1038/ncomms1844](https://doi.org/10.1038/ncomms1844).
- Mehdiabadi NJ, Schultz TR.** 2010. Natural history and phylogeny of the fungus-farming ants (Hymenoptera: Formicidae: Myrmicinae: Attini). *Myrmecological News* **13**:37–55.
- Meyer ST, Leal IR, Tabarelli M, Wirth R.** 2011. Ecosystem engineering by leaf-cutting ants: nests of *Atta cephalotes* drastically alter forest structure and microclimate. *Ecological Entomology* **36**:14–24 DOI [10.1111/j.1365-2311.2010.01241.x](https://doi.org/10.1111/j.1365-2311.2010.01241.x).
- Meyer ST, Neubauer M, Sayer EJ, Leal IR, Tabarelli M, Wirth R.** 2013. Leaf-cutting ants as ecosystem engineers: topsoil and litter perturbations around *Atta cephalotes* nests reduce nutrient availability. *Ecological Entomology* **38**:497–504 DOI [10.1111/een.12043](https://doi.org/10.1111/een.12043).
- Morgulis A, Coulouris G, Raytselis Y, Madden TL, Agarwala R, Schäffer AA.** 2008. Database indexing for production MegaBLAST searches. *Bioinformatics* **24**:1757–1764 DOI [10.1093/bioinformatics/btn322](https://doi.org/10.1093/bioinformatics/btn322).
- Muchovej JJ, Della Lucia TMC.** 1990. Escovopsis, a new genus from leaf cutting ant nests to replace *Phialocladius* nomen invalidum. *Mycotaxa* **37**:191–195.
- Mueller UG, Dash D, Rabeling C, Rodrigues A.** 2008. Coevolution between attine ants and actinomycete bacteria: a reevaluation. *Evolution* **62**:2894–2912 DOI [10.1111/j.1558-5646.2008.00501.x](https://doi.org/10.1111/j.1558-5646.2008.00501.x).
- Mueller UG, Ishak HD, Bruschi SM, Smith CC, Herman JJ, Solomon SE, Mikheyev AS, Rabeling C, Scott JJ, Cooper M, Rodrigues A, Ortiz A, Brandão CRF, Lattke JE, Pagnocca FC, Rehner SA, Schultz TR, Vasconcelos HL, Adams RMM, Bollazzi M, Clark RM, Himler AG, LaPolla JS, Leal IR, Johnson RA, Roces F, Sosa-Calvo J, Wirth R, Bacci M.** 2017. Biogeography of mutualistic fungi cultivated by leafcutter ants. *Molecular Ecology* **26**:6921–6937 DOI [10.1111/mec.14431](https://doi.org/10.1111/mec.14431).
- Mueller UG, Kardish MR, Ishak HD, Wright AM, Solomon SE, Bruschi SM, Carlson AL, Bacci M.** 2018. Phylogenetic patterns of ant–fungus associations indicate that farming strategies, not only a superior fungal cultivar, explain the ecological success of leafcutter ants. *Molecular Ecology* **27**:2414–2434 DOI [10.1111/mec.14588](https://doi.org/10.1111/mec.14588).
- Mueller UG, Rehner SA, Schultz TR.** 1998. The evolution of agriculture in ants. *Science* **281**:2034–2038 DOI [10.1126/science.281.5385.2034](https://doi.org/10.1126/science.281.5385.2034).
- Mueller UG, Wcislo WT.** 1998. Nesting biology of the fungus-growing ant *Cyphomyrmex longiscapus* Weber (Attini Formicidae). *Insectes Sociaux* **45**:181–189.
- Nguyen LT, Schmidt HA, Von Haeseler A, Minh BQ.** 2015. IQ-TREE: a fast and effective stochastic algorithm for estimating maximum-likelihood phylogenies. *Molecular Biology and Evolution* **32**:268–274 DOI [10.1093/molbev/msu300](https://doi.org/10.1093/molbev/msu300).
- Nolasco M, Biondi I, Pimenta DC, Branco A.** 2018. Extraction and preliminary chemical characterization of the venom of the spider wasp *Pepsis decorata* (Hymenoptera: Pompilidae). *Toxicon* **150**:74–76 DOI [10.1016/j.toxicon.2018.04.023](https://doi.org/10.1016/j.toxicon.2018.04.023).

- Nygaard S, Hu H, Li C, Schiøtt M, Chen Z, Yang Z, Xie Q, Ma C, Deng Y, Dikow R, Rabeling C, Nash DR, Wcislo WT, Brady SG, Schultz TR, Zhang G, Boomsma JJ. 2016. Reciprocal genomic evolution in the ant-fungus agricultural symbiosis. *Nature Communications* 7:1–9 DOI 10.1038/ncomms12233.
- Oksanen J, Blanchet FG, Friendly M, Kindt R, Legendre P, McGlinn D, Minchin PR, O’Hara RB, Simpson GL, Solymos P, Stevens MHH, Szoecs E, Wagner H. 2019. vegan: community ecology package. Available at <https://github.com/vegadevs/vegan>.
- Pérez-Ortega B, Fernández-Marín H, Loíacono MS, Galgani P, Wcislo WT. 2010. Biological notes on a fungus-growing ant, *Trachymyrmex* cf. *zeteiki* (Hymenoptera, Formicidae, Attini) attacked by a diverse community of parasitoid wasps (Hymenoptera, Diapriidae). *Insectes Sociaux* 57:317–322 DOI 10.1007/s00040-010-0086-1.
- Persoon CH. 1794. Neuer Versuch einer systematischen Eintheilung der Schwämme. *Neues Magazin Für Die Botanik* 1:63–80.
- Péter A. 2017. Solomon Coder. Available at <https://solomon.andraspeter.com/>.
- Rabeling C, Cover SP, Johnson RA, Mueller UG, Robert J, Mueller UG. 2007. A review of the North American species of the fungus-gardening ant genus *Trachymyrmex* (Hymenoptera: Formicidae). *Zootaxa* 53:1–53 DOI 10.11646/zootaxa.1664.1.1.
- Rabeling C, Schultz TR, Bacci M, Bollazzi M. 2015. *Acromyrmex charruanus*: a new inquiline social parasite species of leaf-cutting ants. *Insectes Sociaux* 62:335–349 DOI 10.1007/s00040-015-0406-6.
- Rambaut A. 2016. FigTree. Available at <https://github.com/rambaut/figtree/releases>.
- R Core Team. 2017. R: a language and environment for statistical computing. Available at <https://www.r-project.org/>.
- Ronque MUV, Feitosa RM, Oliveira PS. 2019. Natural history and ecology of fungus-farming ants: a field study in Atlantic rainforest. *Insectes Sociaux* 66:375–387 DOI 10.1007/s00040-019-00695-y.
- Sánchez-Peña SR, Chacón-Cardosa MC, Canales-del Castillo R, Ward L, Resendez-Pérez D. 2017. A new species of *Trachymyrmex* (Hymenoptera, Formicidae) fungus-growing ant from the Sierra Madre Oriental of northeastern Mexico. *ZooKeys* 2017:73–94 DOI 10.3897/zookeys.706.12539.
- Sanetra M, Crozier RH. 2003. Patterns of population subdivision and gene flow in the ant *Nothomyrmecia macrops* reflected in microsatellite and mitochondrial DNA markers. *Molecular Ecology* 12:2281–2295 DOI 10.1046/j.1365-294X.2003.01900.x.
- Sanllorente O, Ruano F, Tinaut A. 2015. Large-scale population genetics of the mountain ant *Proformica longiseta* (Hymenoptera: Formicidae). *Population Ecology* 57:637–648 DOI 10.1007/s10144-015-0505-2.
- Schlick-Steiner BC, Steiner FM, Seifert B, Stauffer C, Christian E, Crozier RH. 2010. Integrative taxonomy: a multisource approach to exploring biodiversity. *Annual Review of Entomology* 55:421–438 DOI 10.1146/annurev-ento-112408-085432.
- Schultz TR, Bekkevold D, Boomsma JJ. 1998. *Acromyrmex insinuator* new species: an incipient social parasite of fungus-growing ants. *Insectes Sociaux* 45:457–471 DOI 10.1007/s000400050101.

- Schultz TR, Brady SG.** 2008. Major evolutionary transitions in ant agriculture. *Proceedings of the National Academy of Sciences of the United States of America* **105**:5435–5440 DOI [10.1073/pnas.0711024105](https://doi.org/10.1073/pnas.0711024105).
- Schultz TR, Meier R.** 1995. A phylogenetic analysis of the fungus-growing ants (Hymenoptera: Formicidae: Attini) based on morphological characters of the larvae. *Systematic Entomology* **20**:337–370 DOI [10.1111/j.1365-3113.1995.tb00100.x](https://doi.org/10.1111/j.1365-3113.1995.tb00100.x).
- Schultz TR, Solomon SA, Mueller UG, Villesen P, Boomsma JJ, Adams RMM, Norden B.** 2002. Cryptic speciation in the fungus-growing ants *Cyphomyrmex longiscapus* Weber and *Cyphomyrmex muelleri* Schultz and Solomon, new species (Formicidae, Attini). *Insectes Sociaux* **49**:331–343 DOI [10.1007/PL00012657](https://doi.org/10.1007/PL00012657).
- Schultz TR, Sosa-Calvo J, Brady SG, Lopes CT, Mueller UG, Bacci M, Vasconcelos HL.** 2015. The most relictual fungus-farming ant species cultivates the most recently evolved and highly domesticated fungal symbiont species. *The American Naturalist* **185**:693–703 DOI [10.1086/680501](https://doi.org/10.1086/680501).
- Shik JZ, Kooij PW, Donoso DA, Santos JC, Gomez EB, Franco M, Crumière AJJ, Arnan X, Howe J, Wcislo WT, Boomsma JJ.** 2021. Nutritional niches reveal fundamental domestication trade-offs in fungus-farming ants. *Nature Ecology and Evolution* **5**:122–134 DOI [10.1038/s41559-020-01314.x](https://doi.org/10.1038/s41559-020-01314.x).
- Simon C, Frati F, Beckenbach A, Crespi B, Liu H, Flook .** 1994. Evolution, weighting, and phylogenetic utility of mitochondrial gene sequences and a compilation of conserved polymerase chain reaction primers. *Annals of the Entomological Society of America* **87**:651–701 DOI [10.1093/aesa/87.6.651](https://doi.org/10.1093/aesa/87.6.651).
- Singer R.** 1986. *The Agaricales in modern taxonomy*. Koenigstein, Federal Republic of Germany: Koeltz Scientific Books.
- Solomon SE, Rabeling C, Sosa-Calvo J, Lopes CT, Rodrigues A, Vasconcelos HL, Bacci M, Mueller UG, Schultz TR.** 2019. The molecular phylogenetics of *Trachymyrmex* Forel ants and their fungal cultivars provide insights into the origin and coevolutionary history of ‘higher-attine’ ant agriculture. *Systematic Entomology* **44**:939–956 DOI [10.1111/syen.12370](https://doi.org/10.1111/syen.12370).
- Sosa-Calvo J, Ješovník A, Okonski E, Schultz TR.** 2015. Locating, collecting, and maintaining colonies of fungus-farming ants (Hymenoptera: Myrmicinae: Attini). *Sociobiology* **62**:300–320 DOI [10.13102/sociobiology.v62i2.300-320](https://doi.org/10.13102/sociobiology.v62i2.300-320).
- Sosa-Calvo J, Ješovník A, Vasconcelos HL, Bacci M, Schultz TR.** 2017. Rediscovery of the enigmatic fungus-farming ant *Mycetosoritis asper* Mayr (Hymenoptera: Formicidae): implications for taxonomy, phylogeny, and the evolution of agriculture in ants. *PLOS ONE* **12**:1–29 DOI [10.1371/journal.pone.0176498](https://doi.org/10.1371/journal.pone.0176498).
- Sosa-Calvo J, Schultz TR.** 2010. Three remarkable new fungus-growing ant species of the genus *Myrmicocrypta* (Hymenoptera: Formicidae), with a reassessment of the characters that define the genus and its position within the attini. *Annals of the Entomological Society of America* **103**:181–195 DOI [10.1603/AN09108](https://doi.org/10.1603/AN09108).
- Sosa-Calvo J, Schultz TR, Ješovník A, Dahan RA, Rabeling C.** 2018. Evolution, systematics, and natural history of a new genus of cryptobiotic fungus-growing ants. *Systematic Entomology* **43**:549–567 DOI [10.1111/syen.12289](https://doi.org/10.1111/syen.12289).

- Tschinkel WR, Seal JN.** 2016. Bioturbation by the fungus-gardening ant, *Trachymyrmex septentrionalis*. *PLOS ONE* 11:1–15 DOI [10.1371/journal.pone.0158920](https://doi.org/10.1371/journal.pone.0158920).
- Turney S, Cameron ER, Cloutier CA, Buddle CM.** 2015. Non-repeatable science: assessing the frequency of voucher specimen deposition reveals that most arthropod research cannot be verified. *PeerJ* 3:1–19 DOI [10.7717/peerj.1168](https://doi.org/10.7717/peerj.1168).
- Vaidya G, Lohman DJ, Meier R.** 2011. Cladistics multi-gene datasets with character set and codon information. *Cladistics* 27:171–180.
- Vasconcelos HL, Araújo BB, Mayhé-Nunes AJ.** 2008. Patterns of diversity and abundance of fungus-growing ants (Formicidae: Attini) in areas of the Brazilian Cerrado. *Revista Brasileira de Zoologia* 25:445–450 DOI [10.1590/S0101-81752008000300009](https://doi.org/10.1590/S0101-81752008000300009).
- Villesen P, Murakami T, Schultz TR, Boomsma JJ.** 2002. Identifying the transition between single and multiple mating of queens in fungus-growing ants. *Proceedings of the Royal Society London B Biology* 269:1541–1548 DOI [10.1098/rspb.2002.2044](https://doi.org/10.1098/rspb.2002.2044).
- Wang Y, Wang B, Shao X, Shao J, Liu M, Wang M, Wang L.** 2019. The effect of rearing density on immune responses of hepatopancreas and intestine in *Litopenaeus vannamei* against *Vibrio paraheamolyticus* E1 challenge. *Fish and Shellfish Immunology* 93:517–530 DOI [10.1016/j.fsi.2019.08.004](https://doi.org/10.1016/j.fsi.2019.08.004).
- Ward PS, Brady SG, Fisher BL, Schultz TR.** 2015. The evolution of myrmicine ants: phylogeny and biogeography of a hyperdiverse ant clade (Hymenoptera: Formicidae). *Systematic Entomology* 40:61–81 DOI [10.1111/syen.12090](https://doi.org/10.1111/syen.12090).
- Weber NA.** 1940. The biology of the fungus-growing ants. Part VI. Key to *Cyphomyrmex*, new Attini and a new guest ant. *Revista de Entomologia, Rio de Janeiro*: 11:406–427 DOI [10.5281/zenodo.25008](https://doi.org/10.5281/zenodo.25008).
- Weber NA.** 1958a. Evolution in fungus-growing ants. *Proceedings of the Tenth International Congress of Entomology* 2:459–473.
- Weber NA.** 1958b. Nomenclatural changes in *Trachymyrmex* (Hym.: Formicidae, Attini). *Entomological News* 69:49–55.
- Weber NA.** 1972. Gardening ants, the attines. *Memoirs of the American Philosophical Society* 92:1–146.
- Wheeler WM.** 1903. A decade of Texan Formicidae. *Psyche* 10:93–111 DOI [10.1155/1903/67840](https://doi.org/10.1155/1903/67840).
- Zhang Z, Schwartz S, Wagner L, Miller W.** 2000. A greedy algorithm for aligning DNA sequences. *Journal of Computational Biology* 7:203–214 DOI [10.1089/10665270050081478](https://doi.org/10.1089/10665270050081478).